*Digital Comprehensive Summaries of Uppsala Dissertations*
*from the Faculty of Science and Technology 2329*

# Investigating ageing mechanisms in electric vehicle batteries

## *A multiscale approach to material analysis*

ANASTASIIA MIKHEENKOVA



ACTA UNIVERSITATIS
UPSALIENSIS
2023

ISSN 1651-6214
ISBN 978-91-513-1939-1
urn:nbn:se:uu:diva-514588

UPPSALA
UNIVERSITET

Dissertation presented at Uppsala University to be publicly examined in 101195, Heinz-Otto Kreiss, Ångströmlaboratoriet, Lägerhyddsvägen 1, Uppsala, Thursday, 7 December 2023 at 09:15 for the degree of Doctor of Philosophy. The examination will be conducted in English. Faculty examiner: Professor Sandrine Lyonnard (CEA-IRIG).

**Abstract**
Mikheenkova, A. 2023. Investigating ageing mechanisms in electric vehicle batteries. A multiscale approach to material analysis. *Digital Comprehensive Summaries of Uppsala Dissertations from the Faculty of Science and Technology* 2329. 84 pp. Uppsala: Acta Universitatis Upsaliensis. ISBN 978-91-513-1939-1.

Electrifying passenger transport is a key strategy in combating global warming, with Li-ion batteries (LIBs) being the current go-to technology. Despite LIB's satisfactory performance and carbon-neutral operation, lifetime and safety are still public concerns. A thorough understanding of battery ageing is crucial for improving LIBs and advancing the overall sustainability of LIB technology. This thesis bridges a gap between academic and industrial research by combining commercial battery investigation with a multiscale approach using a combination of in-house and synchrotron characterization methods used with the implementation of method development to study commercial batteries.

The multiple degradation mechanisms were identified at various scales in the aged commercial cells. Specifically, the results show that the studied cells exhibit significant and distinct ageing heterogeneity in prismatic and cylindrical cell formats, where the area with the highest degradation is found on the side of the positive tab, where the current and temperature gradients are expected to be the strongest. After decoupling the performance on the electrode level, the Ni-rich layered oxide positive electrodes show a significant increase in $Li^+$ diffusion resistance in the aged materials as a function of the State of Charge (SoC) range and temperature. Furthermore, heterogeneity is an issue relevant also on a secondary particle scale, where identified SoC gradients ranging from the centre to the surface of the particle might induce kinetic limitations and cause an increase in Li+ diffusion resistance. On a single particle level, the formation of a large number of voids within the grains was found. Such degradation can additionally contribute to the resistance increase in the material by changing tortuosity for Li-ions. Finally, at the atomic level, Ni was found to be the dominant charge compensator, which can decrease up to 25% of the redox activity after ageing. Compared to Ni, Co was found to be less redox-active, but more involved in charge compensation through changes in hybridization with the oxygen atom. The oxygen, in turn, was revealed to participate in anionic redox reactions at low SoC by both hybridization to TM and also through the formation of molecular oxygen at lower potentials than previously reported. The observed decrease in oxygen anion redox activity follows with material losing performance.

The results presented in the thesis demonstrate the importance of the multiscale approach in order to form a more complete understanding of the degradation processes which have effects within different scales.

*Keywords:* Li-ion batteries, Ni-rich cathode, Ageing mechanisms, Batteries for electric vehicles, X-ray diffraction, NCA, NMC811

*Anastasiia Mikheenkova, Department of Chemistry - Ångström, Structural Chemistry, Box 538, Uppsala University, SE-751 21 Uppsala, Sweden.*



ISSN 1651-6214
ISBN 978-91-513-1939-1
URN urn:nbn:se:uu:diva-514588 (http://urn.kb.se/resolve?urn=urn:nbn:se:uu:diva-514588)

*To Anna and Eduard,*
*who taught me that success is not a solitary pursuit, but a team effort.*
*You have been not just any team, but the very best one could hope for.*

# List of Papers

This thesis is based on the following papers, which are referred to in the text by their Roman numerals.

I. **Mikheenkova, A.**, Smith, A. J., Frenander, K. B., Tesfamhret, Y., Chowdhury, N. R., Tai, C.-W., Thiringer, T., Lindström, R. W., Hahlin, M., & Lacey, M. J. (2023). Ageing of high energy density automotive Li-ion batteries: The effect of temperature and state-of-charge. *Journal of The Electrochemical Society*, *170*(8), 080503.

II. **Mikheenkova, A.**, Schökel, A., Smith, A. J., Ahmed, I., Brant, W. R., Lacey, M. J. & Hahlin, M. Visualizing Ageing-Induced Heterogeneity Within Large Prismatic Lithium-Ion Batteries for Electric Cars Using Diffraction Radiography. *Submitted.*

III. **Mikheenkova, A.**, Chen, H., Chen, H., Dzhigaev, D., Sjö, H., Kalbfleisch, S., Brant W.R., Wallentin, J. & Hahlin, M. Revealing Secondary Particle Heterogeneity in Ni-rich NCA Secondary Particles in Electric Car Battery Material. *In manuscript.*

IV. **Mikheenkova, A.**, Gustafsson, O., Misiewicz, C., Brant, W. R., Hahlin, M., & Lacey, M. J. (2023). Resolving high potential structural deterioration in Ni-rich layered cathode materials for lithium-ion batteries Operando. *Journal of Energy Storage*, *57*, 106211.

V. **Mikheenkova, A.**, Mukherjee, S., Hirsbrunner, M., Törnblom, P., Tai, C.-W., Segre, C. U., Ding, Y., Zhang, W., Asmara, T. C., Wei, Y., Schmitt, T., Rensmo, H., Duda, L. & Hahlin, M. (2023). The Role of Oxygen in Automotive Grade Lithium-Ion Battery Cathodes: An Atomistic Survey of Ageing. *Submitted*.

VI. **Mikheenkova, A.**, Liu, Q., Azmi, R., Ciambezi, M., Ramakrishnan, M., Mukherjee, S. & Hahlin, M. Ageing makes a difference: operando observations of Ni and Co chemical states in aged electrodes from automotive cells. *In manuscript*.

VII. Hirsbrunner, M., **Mikheenkova, A.**, Törnblom, P., Mukherjee, S., Schmitt, T., House, R., Rensmo, H., Hahlin, M. & Duda, L. Vibrationally-resolved RIXS reveals OH-group formation in oxygen redox active Li-ion battery cathodes. *In manuscript*.

Reprints were made with permission from the respective publishers.

# Comments on the Author's Contribution to the Papers

I. Coordinated post-mortem measurements. Planned, performed and analysed most of the *post-mortem* material characterization measurements. Took part in sample preparation, data collection and analysis of transmission electron microscopy measurements. Performed and analysed part of electrochemical measurements. Wrote the manuscript with input from the co-authors.

II. Planned and coordinated the measurements with input from the co-authors. Conducted radiography diffraction measurements with the assistance from the beamline scientist. Analysed radiography measurements. Took part in conducting and analysing electrochemical measurements. Wrote the manuscript with input from the co-authors.

III. Planned and coordinated the project with input from the co-authors. Prepared materials and performed assembly of the battery cells for *operando* measurements. Conducted experiment with input from the co-authors and support from the beamline scientist. Performed and analysed *operando* and electrochemical measurements. Wrote the manuscript with input from the co-authors.

IV. Coordinated and prepared materials for *operando* measurements. Performed X-ray diffraction measurements. Analysed electrochemical measurements from all experiments. Wrote the manuscript with input from the co-authors.

V. Planned and coordinated the project together with co-authors. Planned and coordinated measurements with co-authors. Prepared material for all synchrotron measurements. Took part in sample preparation, data collection and analysis of transmission electron microscopy measurements. Wrote the manuscript together with co-authors.

VI. Planned and coordinated the project with input from the co-authors. Planned experiments with input from the co-authors. Prepared material and performed assembly of the battery cells for *operando*

measurements. Conducted X-ray absorption spectroscopy measurements with the assistance from the beamline scientists and co-authors. Analysed *operando* XAS and electrochemical measurements with input from the co-authors. Wrote the manuscript with input from the co-authors.

VII. Planned and coordinated measurements with co-authors. Prepared material for all measurements. Contributed to the manuscript writing.

# Extended bibliography

The author contributed to the following publications that are not included in the present thesis:

1. Smith, A. J., Fang, Y., **Mikheenkova, A.**, Ekström, H., Svens, P., Ahmed, I., Lacey, M.J., Lindbergh, G., Furó, I. & Wreland Lindström, R. (2023) Localized lithium plating under mild cycling conditions in high-energy lithium-ion batteries. *Journal of Power Sources*, 573, 233118.

2. Chowdhury, N.R., Smith, A.J., Frenander, K., **Mikheenkova, A.**, Wreland Lindström & R., Thiringer, T. The state of charge dependence of degradation in lithium-ion cells from a Tesla Model 3. *Submitted*.

3. Chen, H., Ericson, T., Temperton, R., Källquist, I., Liu, H., Eads, C.N., **Mikheenkova, A.**, Andersson, M., Kokkonen, E., Brant, W. R. & Hahlin, M. Investigating surface reactivity of a Ni-rich cathode material towards CO2, $H_2O$, and $O_2$ using ambient pressure X-ray photoelectron spectroscopy. *Accepted*.

4. Maltoni, P., Barucca, G., Rutkowski, B., Spadaro, M.C., Ivanov, S.A., Yaacoub, N., **Mikheenkova, A.**, Ek, G., Eriksson, M., Almqvist, B., Varvaro, G., Sarkar, T., De Toro, J.A., Peddis, D. & Mathieu, R. Engineering. Hard Ferrite Composites by Combining Nanostructuring and $Al^{3+}$ Substitution: from Nano to Dense Bulk Magnets, *In Preprint*.

# Contents

# Abbreviations and field specific terms

## Abbreviations

DEC – Diethyl Carbonate
DESY – Deutsches Elektronen-Synchrotron
DMC – Dimethyl Carbonate
DoD – Depth of Discharge
DVA – Differential Voltage Analysis
EC – Ethylene Carbonate
EDX – Energy Dispersive X-ray Spectroscopy
EMC – Ethyl Methyl Carbonate
EoL – End of Life
EV – Electric Vehicle
EU – European Union
EXAFS –Extended X-ray Absorption Fine Structure
ICA – Incremental Capacity Analysis
ICI – Intermittent Current Interruption
ICP-OES – Inductively Coupled Plasma Optical Emission Spectroscopy
LAM – Loss of Active Material
LCO – $LiCoO_2$
LIB – Li-ion battery
LDV – Light Duty Vehicles
LFP – $LiFePO_4$
LLI – Loss of Lithium Inventory
LMO – $LiMnO_2$
LiTMO – Lithiated transition metal oxide
LNO – $LiNiO_2$
NCA – $LiNi_{1-x-y}Al_xCo_yO_2$
NHE – Normal Hydrogen Electrode
NMC – $LiNi_{1-x-y}Co_xMn_yO_2$
NMP – N-Methyl-2-pyrrolidone
PC – propylene carbonate
RI – Resistance Increase
RIXS – Resonant Inelastic X-ray Scattering
ROI – Region of Interest
SEI – Solid Electrolyte Interphase
SEM – Scanning Electron Microscopy

SDGs – Sustainable Development Goals
SoC – State of Charge
SoH – State of Health
TM – Transition Metal
XANES – X-ray Absorption Near Edge Structure
XAS – X-ray Absorption Spectroscopy
XRD – X-ray Diffraction

# Glossary

Depth of Discharge (DoD) - The discharged capacity of a battery related to the maximum capacity, %
Energy Density - The nominal battery energy per unit of measure. In case of mass can be also used as gravimetric energy density and in case of volume it is referred as to energy density, Wh/kg or Wh/L
Internal resistance - The opposition to the current by internal cell components, measured as relationship of the cell potential to the draw current, Ω
Nominal capacity - The total amount of charge, which can be received from a battery discharged from 100% State of Charge to 0% State of Charge at a certain discharge current, Ah
Nominal voltage - The amount of voltage output a cell gives out when charged, V
State of Charge (SoC) - Battery capacity expressed in % where full capacity corresponds to 100%, %
State of Health (SoH) - A unit describing condition of a battery compared to its beginning of life conditions. Often expressed as percentage of capacity retention compared to its initial capacity, %

# List of symbols

$E$ – Potential, V
$k$ – diffusion resistance coefficient, Ω $s^{-0.5}$
$R$ – Internal resistance, Ω
$t$ – time, s
$V$ – Voltage, V
$Q$ – Capacity, mAh
Θ – diffraction angle, °
π – mathematical constant equal to 3.14159
σ – Warburg parameter, Ω

# 1. Introduction

## 1.1 The future is electric

### 1.1.1 Automotive electrification in climate action

In the urgent battle against climate change, the world races against time, striving to mitigate the severe consequences of global warming that humanity is already beginning to endure.[1,2] Global warming is traced back to the latter half of the 19th century, tied to the Industrial Revolution, which significantly amped up human activities like coal burning.[3] Although the concept that Earth's atmosphere contains heat-insulating materials was introduced earlier, in the beginning of the 19th century by Joseph Fourier,[4] it was not until 1896 that Svante Arrhenius predicted how atmospheric carbon affects Earth's surface temperature via the greenhouse effect.[5]

Concerns regarding global warming significantly increased towards the end of the 20$^{th}$ century, culminating in the establishment of the United Nations Framework Convention which came into effect in 1994, followed by the Kyoto Protocol, endorsed by 192 countries in 1997.[6] Nearly two decades later, escalating evidence of unavoidable climate change resulted in the Katowice Climate Package at the UN Climate Change Conference, aiming to limit global warming to 2.0 °C.[7] This package outlines essential regulations to decrease greenhouse emissions and tackle the repercussions of global warming. The European Union's (EU) sustainable development strategies were summarized in the Sustainable Development Goals (SDGs), a 2030 agenda adopted by the United Nations.[8] In accordance with the SDGs, transport decarbonization will reduce the greenhouse gas load on the environment.[9]

The road vehicles are currently responsible for 15% of the total EU emissions of $CO_2$.[9] The new regulations aim to ensure that all new cars and trucks placed on the market from 2035 onwards will be zero-emission vehicles, as a mitigation strategy for reducing the carbon footprint of these vehicles.[9] The zero-emission transport market is anticipated to be largely dominated by electric vehicles (EVs) in the future.[10] There are several types of electric vehicles currently available on the market: Plug-In Hybrid Electric Vehicles, Hybrid Electric Vehicles, Range Extenders, Fuel Cell Vehicles, and Battery Electric Vehicles.[11] All EVs require a battery to operate.

## 1.1.2 From lead to lithium

The first EV prototype was invented more than 150 years ago, rapidly gaining popularity between 1880 and 1900, a period later called by historians as *the golden age* of EVs.[12,13] Even back then, inventors were driven by concerns regarding the smoke and pollution emitted from factories and considered battery-powered vehicles an optimal solution. EVs were powered by lead-acid batteries, which is the first commercial rechargeable battery, which had been invented a couple of decades prior.[14] However, before long, steam and gasoline-driven engines began to emerge as strong market competitors due to their lower prices and higher driving ranges.[12,15] Only in the 2020s did the combined call for climate action and the rapid development of Li-ion batteries (LIBs) result in a rapid expansion of the battery-powered EV market.[16]

The battery in an electric vehicle has several requirements: safe usage, performance with minimal impact on and from the environment, an operating life of around 15 years, low cost, and high energy density.[17] Energy density is often discussed the most as it defines the driving range of the vehicle. Extending the driving range can be achieved by increasing the number of cells used in batteries or by using materials that satisfy the requirements.

Figure 1 (adapted from reference [18]) presents a Ragone plot of various battery technologies. The energy characteristics of different types of batteries are compared in terms of gravimetric energy density (the amount of energy stored per unit mass) *vs* volumetric energy density (the amount of energy stored per unit volume). From this plot, it is evident that Li-ion batteries have significantly advanced beyond the originally used lead-acid batteries. Currently, Li-ion battery is considered a driving technology for the rapid transition to electric vehicles. However, substantial concerns regarding the environment as well as material abundance have led to wide consideration of other chemistries, such as Na-ion, for example.[19,20]

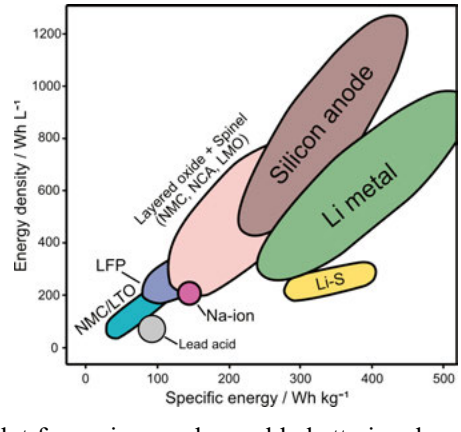


Figure 1 - Ragone plot for various rechargeable batteries showing superiority of the Li-based battery systems as the desired energy devices for electric vehicles. Adapted from reference.[18]

## 1.2 Lithium-ion batteries

The LIB has been claimed as the technology that changed the world. The chemistry Nobel Prize 2019 was awarded to John B. Goodenough, M. Stanley Whittingham and Akira Yoshino for "their contributions to the development of the lithium-ion battery".[21] The first industrial LIB on the market was introduced in 1991 by Sony Co for portable electronics, replacing Ni-Cd chemistry, which has lower energy density and higher environmental impact. Now, 30 years later, LIBs are widespread in EVs, including passenger cars.[13] The current market (as of 2023) of LIB is estimated ~54 B USD and expected to increase at least threefold within the next 7 years.[22] LIB technology plays an essential role in the world, and its importance continues to grow.

The basic components of a lithium-ion battery include the positive electrode, the negative electrode, and the electrolyte (Figure 2). Both the positive and negative electrodes comprise an electrode coating and a current collector. The electrode coating consists of a mixture of active material, conductive carbon, and a binder. The active material participates in electrochemical reactions, serving as a host material for the Li-ions and containing redox centres (atoms that can change their oxidation state by giving or receiving electrons). Conductive carbon enhances electron conductivity within the electrode coating, which is crucial for charge compensation during lithiation and delithiation. The polymer binder maintains the mixture's integrity and ensures the electrode's mechanical flexibility. The electrode coating is applied to a current collector, typically made of copper for the negative electrode and aluminium for the positive electrode. The electrolyte is a solution that facilitates the movement of lithium ions between the electrodes while maximizing electrical isolation. In all conventional battery types, a separator is required and is placed between the positive and negative electrodes to prevent contact and short-circuiting of the battery.

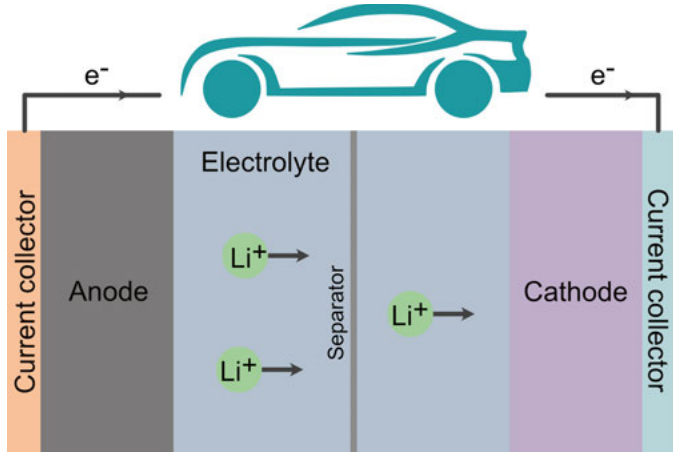


Figure 2 – LIB working principle.

The simplified working principle of the LIB can be summarized as following: under a load, lithium ions move from the negative electrode to the positive electrode due to a spontaneous reaction (Figure 2). This movement is accompanied by the flow of electrons as current through the current collector, supplying power to the connected device. This process is called discharge. During charging, electrical energy is supplied to the system, which, through the reversed redox reactions, is converted and stored as chemical energy. During the process, Li-ions move from the positive electrode to the negative electrode through the electrolyte. This process can be also described as the delithiation of the positive electrode and the lithiation of the negative electrode.

The example of the processes inside the battery material for an intercalation battery with graphite as the negative electrode and lithiated transition metal oxide (LiTMO) as the positive electrode summarized in electrochemical reactions on the negative electrode (1) and positive electrode (2) as well as full cell reaction (3) below:

$$nC + xLi^+ + xe^- \rightleftarrows Li_xC_n \quad (1)$$

$$LiTMO_2 \rightleftarrows Li_{1-x}TMO_2 + xLi^+ + xe^- \quad (2)$$

$$nC + LiTMO_2 \rightleftarrows Li_{1-x}TMO_2 + Li_xC_n \quad (3)$$

The driving force for the movement of Li-ions is the difference in potential between the positive and negative electrodes. In the current work, all potentials discussed are referenced to $Li/Li^+$ as it is considered a standard in the field.

The voltage is defined by the difference in electrochemical potential between the negative and the positive electrodes. The capacity of a material is dependent on the amount of lithium that can be reversible extracted or inserted in the active material. The theoretical capacity is defined as number of the reactive electrons to the molar weight of the material.[23] The energy of the redox couples set the limit to the voltage of the materials.[24]

There is a number of terms typical for describing the properties of the battery. The section “Abbreviations and field specific terms” lists the key terms important to describe a battery performance used later in the text.

## 1.3 Materials for LIBs

Figure 3 (adapted from reference[25]) illustrates some of the most used chemistries for the positive and the negative electrodes. The general requirements for materials currently in use include high power and energy density, acceptable safety levels, utilization of abundant elements, and low cost. Ultimately, the choice of materials represents a trade-off among various properties to satisfy

the battery application. Battery energy is a crucial characteristic of the system, defined by the material's potential and its capacity. Figure 3 presents the most common positive and negative electrode chemistries in LIBs. Maximizing both potential and capacity, from the perspective of the negative electrode, can be achieved using Li metal. However, this is currently considered challenging as Li metal is prone to dendrite formation—a problem believed to be mitigated with the introduction of solid-state batteries to a significant extent.[26] From the positive electrode point, transition metal (TM) oxides are believed to be the optimal solution. The negative electrode is dominated by graphite with Si chemistries also gaining popularity.[27–30] The research suggests improvements to capacity and potential by proposing, for example, Li-rich[31–33] and high-voltage cathodes.[34] However, the stability of these materials does not permit their current use on the market.

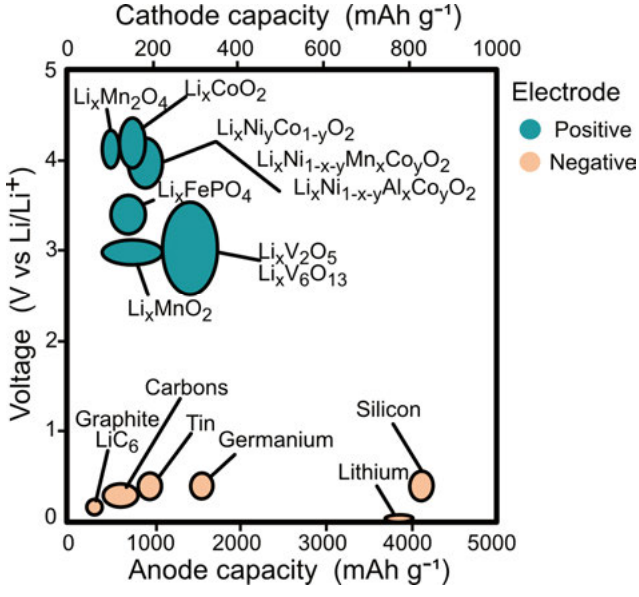


Figure 3 - Potential *vs*. capacity for typical lithium ion anode and cathode materials. Adapted from reference.[25]

Ni-rich cathode materials, such as $LiNi_{1-x-y}Co_xMn_yO_2$ (NMC) or $LiNi_{1-x-y}Al_xCo_yO_2$ (NCA) with Ni content exceeding 60%, are superior due to their higher capacity and energy density. Figure 4 (adapted from reference[16]) summarizes the most common cathode chemistries in the newly produced light duty vehicles (LDV) market between 2018 and 2022. Notably, $LiFePO_4$ (LFP) starts to increase its share in the market. LFP, a material utilizing more abundant resources, is gaining traction with the aid of research aimed at overcoming intrinsic material challenges, such as poor electron conductivity and blockage of Li-ion diffusion channels.[35] As the EV market shifts its focus towards prioritizing fast charging over battery capacity, LFP has advantage over some of

the chemistries. However, the TM oxide cathodes show significant outperformance and are predicted to keep dominating on the EV market with Ni-rich based chemistries remain highly represented.[36]

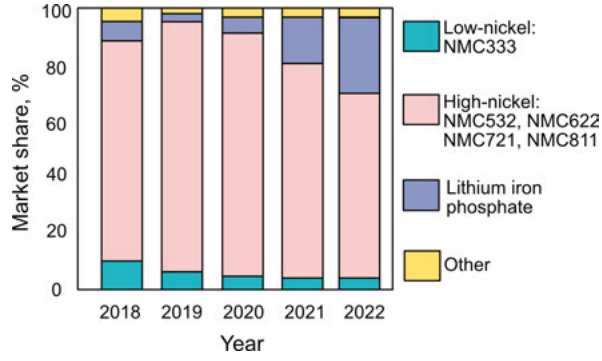


Figure 4 – Chemistry of the positive electrode used in LDV. Adapted from reference.[16]

## 1.3.1 Ni-rich transition metal oxides as positive electrode active materials

The journey of layered oxide cathodes began with the discovery of $LiCoO_2$ (LCO) by Professor John B. Goodenough[37,38] in 1980. This milestone was followed by the discovery of $LiNiO_2$ (LNO), which increased achievable capacity. However, the structural instability of LNO necessitated the introduction of additional elements such as Mn, Al, Si, Fe, Ti, W, *etc*.[39]

An intermediate state, $LiNi_xCo_yMn_zO_2$ (x<60%) has become prevalent in the market in during the beginning of the 21$^{st}$ century. However, the upscaling of the production, the environmental concern together with the cost of Co, its unethical mining and various geopolitical reasons, established a trend on reduction of Co content in the batteries.[40]

The current thesis is focused on Ni-rich layered oxide positive electrode active materials such as NMC and NCA. Ni-rich layered oxide cathodes consist of transition metal and oxygen slabs with lithium sites in between (Figure 5). The material adopts a structure with rhombohedral symmetry (R-3m symmetry point group). The TMs and Li occupy sites with octahedral oxygen coordination. The particles of TM layered oxides are polycrystalline and called secondary particles. The secondary particles, with the diameter ~10-20 µm, consist of single crystals in smaller size (~100 nm) which are called primary particles.[41]

The process of delithiating the TM oxides or analogous material can occur through two pathways: oxygen dumbbell hopping and tetrahedral site hopping.[42] Delithiation of the material is divided into two regions: one within the stability range (<4.25 V) and the other beyond it (>4.25 V).[43] Within the

stability region, Li extraction is largely reversible. During delithiation, changes in the lattice parameters *a* and *c* exhibit differences. The *a* lattice parameter decreases sublinearly with the amount of Li in the structure. In the case of the *c* parameter, it initially increases until it reaches approximately 4.0 V and then starts to decrease. This decrease in the *c* lattice parameter is commonly referred to as "lattice collapse". The general consensus regarding this phenomenon is that during material delithiation, the TM-O bonds gain covalent character, resulting in a decrease in the spacing between oxygen slabs.[44] Under operational conditions, the region associated with maximum reversibility is typically considered to be below approximately 4.2 V.[42]

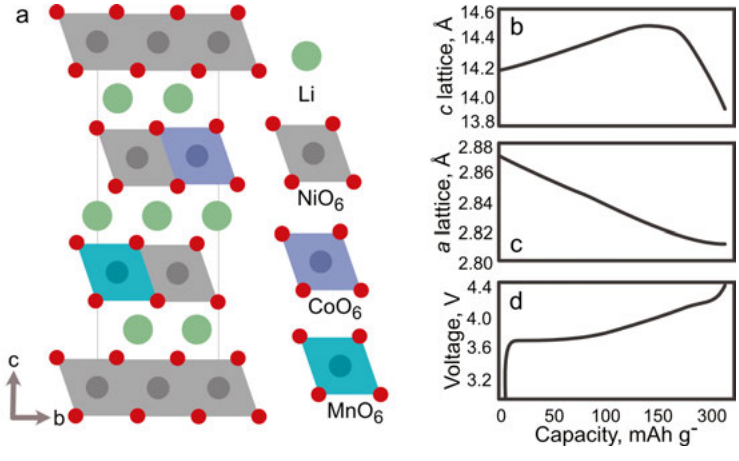


Figure 5 – Crystallographic structure of Ni-rich layered oxide on example of NMC811 (a) and evolution of a and b lattice parameters during battery operation (b and respectively) together with voltage profile (c). Adapted from Reference.[41]

As previously described, during the processes of lithiation and delithiation, the redox centres either release or absorb electrons. The primary mechanism facilitating this is the reduction or oxidation of the transition metals, a process also known as cationic redox. These reactions are governed by energy barriers for lithium diffusion and the electronic structure.[45] However, recent studies highlight that the mechanism behind is more complex and one should account for the oxygen participation (also called anionic redox).[43,46]

Anionic redox is currently extensively discussed in the community.[47–50] In the specific case of TM oxide cathodes, anionic redox means reversible oxygen reduction and oxidation. The oxygen participation was theorised using Lewis configuration of $O^{2-}$. Unlike the previous description of the electronic structure, it proposes that one of the O 2*p* orbitals has a relatively small overlap with Li 2*s*, which results in weak bonding and behaves like O non-bonding state. Such a change offers an additional band for removing electrons, while conserving stability of the structure.[48]

### 1.3.2 Other components of LIBs

The current thesis mainly focuses on the positive electrode. However, other components of the LIBs are described briefly in this chapter. For more detailed information, the following review papers are recommended: [51–53].

#### 1.3.2.1 Graphite-based negative electrode active materials

Graphite is the negative electrode active material for the vast majority of current commercial applications.[13,27] Graphite is a crystalline carbon allotrope whose theoretical capacity of 372 mAh $g^{-1}$ and the potential range for electrochemical cycling is found to be beneficial for applications in electric cars including ones for EVs.

To satisfy high energy density requirements for LIB, graphite-Si composites are present in the market. The specific capacity of 4200 mAh $g^{-1}$ and low electrochemical potential of 0.4 V vs $Li/Li^+$ attract research towards it. However, Si suffers significant volume expansion upon lithiation and delithiation resulting in particle cracking, Li trapping and loss of electrical contact. To benefit from compelling Si properties and yet achieve cycling stability, $SiO_x$ is introduced into the graphite matrix.[28] The current work does not analyse the negative electrode and associated degradation closely.

#### 1.3.2.2 Electrolytes

Electrolyte allows lithium ions to move between cathode and anode. The conventional LIBs use liquid electrolyte. It consists of organic solvent with lithium salts dissolved in it. The general requirements of an electrolyte is ionic conductivity, electrochemical stability, electronic insulation, low cost, wide range of working temperatures and safety.[54,55] The most common composition of the salt is Lithium hexafluorophosphate ($LiPF_6$). Its role is to serve as a solvation shell for Li ions during their transportation through electrolyte. The most common solvents in electrolytes are ethylene carbonate (EC), diethyl carbonate (DEC), dimethyl carbonate (DMC), ethyl methyl carbonate (EMC), and propylene carbonate (PC).[56]

## 1.4 LIBs ageing

Understanding the degradation processes of LIBs is crucial for prolonging battery lifetime and ensuring safety. Additionally, investigating ageing is vital for diagnosing the cells[1] for potential second-life applications or recycling.

The lithium ion battery degradation involves many interdependent processes. The key summary is presented in Figure 6 (reproduced with

[1] A cell is a single unit of the positive and negative electrodes, separator, and electrolyte, while a battery consists of several cells. In the battery field, these terms are sometimes used interchangeably.

permission from Reference[57]), and include ageing processes which happen in the positive and negative electrodes, electrolyte and separator. To simplify the ageing evaluation, the following ageing modes were introduced:

1. **Loss of Lithium Inventory (LLI):** summarizes mechanisms that involve consumption of Li ions (*i.e.* parasitic reactions, decomposition reactions, irreversible lithium plating, lithium trapping, *etc*);
2. **Loss of Active Material (LAM):** summarizes mechanisms that involve loss of positive or negative active material or, in other words, loss of available redox centres or availability to host lithium ions (transition metal dissolution, transition to inactive phases, particle cracking, *etc*);
3. **Resistance Increase (RI):** summarizes degradation mechanisms that lead to increase of the electrical contact resistance or decrease of lithium diffusion and, therefore, loss of power (current collector corrosion, binder decomposition, *etc*).

The degradation modes, being helpful especially for estimation of the battery state for various applications, is a simplification. The same degradation mechanisms can have several impacts: *e.g.* loss of active material being a classical case for LAM can also lead to LLI if there are Li ions trapped inside.

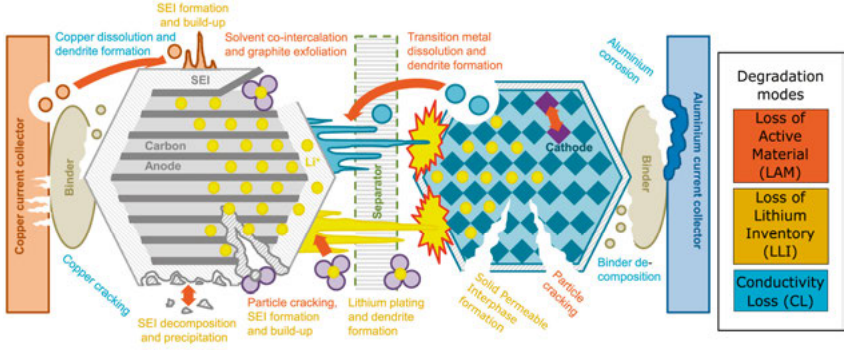


Figure 6 – Summary of Li-ion battery ageing processes. Reproduced with permission from Reference.[57] © 2019 The Authors. Published by Elsevier Ltd.

The summary below describes the most common degradation mechanisms with particular focus on cathodes. The following studies are referred for more in-depth information: [42,58,59].

## 1.4.1 Positive electrode ageing

In automotive applications, the degree of delithiation of the cathode material typically does not exceed ~65%, which is generally defined as the stability limit for Ni-rich layered oxides. However, even within this purportedly stable region, various degradation modes occur. The main focus of this work is on

cathode degradation, which will be elaborated upon in detail in this section. However, ageing of inactive components, *e.g.* binder decomposition, corrosion of current collectors, play significant role.

#### 1.4.1.1 Particle cracking

Particle cracking is considered a major degradation mechanism in TM oxides. The reasons for particle cracking in the materials include heterogeneous phase transition, induced stress, and oxygen evolution during operation.[59] Studies have shown that (a) some of the particle cracking is reversible,[46] and (b) some of the particle cracking was introduced already during the electrode manufacturing, mostly, during calendering.[60] However, the extent of the particle cracking upon ageing is present and considered a strong driver of the material deterioration.

#### 1.4.1.2 Transition metal dissolution

Transition metal dissolution is a parasitic reaction that occurs during battery operation. Transition metals are dissolved from the active material into the electrolyte and can later be found reduced on the negative electrode. The mechanism behind this phenomenon is still under discussion. In the case of NMC811 or other manganese-containing materials, it is typically attributed to disproportionation reactions, such as the instability of $Mn^{3+}$ leading to the formation of $Mn^{2+}$ and $Mn^{4+}$, which are prone to dissolution. Other theories include acidic leaching and oxygen loss. For instance, it is believed that singlet oxygen, released from NMC, oxidizes the electrolyte solvent (*e.g.*, ethylene carbonate) generating water. This, in turn, leads to the hydrolysis of lithium hexafluorophosphate, $LiPF_6$, and the subsequent formation of hydrofluoric acid (HF).[61,62] The reduction of the TMs in the anode is associated with the increase of the resistance, decrease of the Solid Electrolyte Interphase (SEI) quality and capacity fade.[63]

#### 1.4.1.3 Phase transformation

Phase transformation is a common ageing mechanism. Usually, several phenomena are considered: (a) formation of the surface layer, often called surface reconstruction, *e.g.* NiO, which decreases Li diffusion; or (b) irreversible transformation of the part of the material onto electrochemically inactive phase, which fails to accommodate Li at the same capacity or completely.

#### 1.4.1.4 Cation mixing

Cation mixing is a term that refers to the occupation of Li sites by Ni, or the so-called Ni/Li antisites mixing. It is shown that such mixing is introduced during synthesis as it stabilizes the structure.[64] Cation mixing is generally associated with capacity reduction within the material. The effect of Ni introduction into Li sites is twofold: on one hand, it increases the energy barrier for

Li diffusion; on the other hand, it reduces the number of sites which were supposed to host Li-ions.

#### 1.4.1.4 Oxygen and other gases release

As was briefly described before, irreversible release of oxygen was found in the Ni-rich TMO materials. The problem of oxygen release, in addition to losing part of the structure, is the reaction of oxygen with other compounds of the LIB, such as electrolyte. The products of interaction, such as CO and $CO_2$, are typically found at higher operating potentials of the material.[62,65,66]

### 1.4.2 Other component degradation

The thesis is mainly focused on the positive electrode-related processes. However, a short information of degradation of other compounds is presented in this section. For more detailed information, the following articles are recommended:[51,52].

#### 1.4.2.1 Negative electrode ageing

The degradation of the graphite – based negative electrode includes corrosion of current collectors, particle disconnection and fracture, graphite exfoliation, SEI degradation, and Li plating together with the dendrite growth.[59]

SEI degradation is intensely studied, yet, a complex and not well-understood process. SEI is a passivation layer which is located on the negative electrode and it serves for stabilization of the negative electrode – electrolyte interface. The SEI consists of organic and inorganic Li-containing compounds. Its stability is important for long-term battery operation. However, SEI is sensitive towards external impact, *e.g.* temperature, electrode volume change, as well as other degradation mechanisms, *e.g.* TM dissolved from the positive electrode can reduce on the negative electrode and result in the resistance increase.[61,67]

The particle disconnection in graphite is an issue similar to the positive electrode. The mechanisms behind that are typically attributed to the changes in the material volume and stress induced by lithiation/delithiation.[68]

A dissolution of the current collector is also considered a common issue. Cu, unlike Al, which is used on the positive electrode, is vulnerable to acidic corrosion that occurs at high potentials.[69]

Li plating or Li deposition on the negative electrode is another degradation mechanism. Li plating can be triggered by high current, low temperature, high SoC. The deposition is thermodynamically allowed below 0 V *vs* $Li/Li^+$ and it happens when the low number of available vacancy cites for Li intercalations limit $Li^+$ solid state diffusion.[70]

#### 1.4.2.2 Electrolyte

Electrolyte ageing is highly important to consider as it is in contact with all main components of LIB and its degradation influences significantly on the whole system. The degradation of the electrolyte is a complex issue with many interrelated processes. Electrolyte decomposition is dependent on the electrolyte content and used additives.[71]

# 2. Scope of the thesis

The overachieving goal of this work is to understand and connect the degradation mechanisms seen in Li-ion batteries from commercial Electric Vehicles (EVs) under different operational conditions. A particular focus is on the ageing issues of the positive electrode, as seen in NMC811 and NCA chemistries. Ni-rich TM oxides have been studied extensively due to their promising properties, but the degradation pathways of Ni-rich layered oxide materials are still not fully understood. The target of the investigations within this thesis is to delve deeper into the degradation complexity by examining material degradation from commercially used batteries at different scales. Analysing these materials in commercially-relevant form factors can help in understanding battery degradation scenarios close to user conditions. However, commercially obtained batteries make the analysis complex due to their composition, challenging sample preparation, and lack of control over certain studied parameters, which makes precise investigation difficult.

The thesis specifically aims to identify relevant degradation mechanisms in commercial battery cells. The starting point is to understand how the general performance of batteries depends on cycling conditions and to separate the contributions of the positive and negative electrodes. As commercial cells are significantly larger than typical laboratory cells, the question of heterogeneity should be explored by comparing various cell geometries since local accelerated ageing indicates pitfalls in battery design. Further, decoupling the degradation contributions of the positive and negative electrodes is targeted. The differentiation of the ageing consequences on the electrode level can lead to understanding the directions for the improvement of the materials. After, the deteriorations formed upon ageing should be studied within a particle level for possible heterogeneities. Finally, an atomistic analysis is in the scope as the thesis, as understanding of main components operation, *e.g.* lithium, oxygen and transition metal ions, and how they change after ageing, is essential for improving battery functionality.

To explore LIBs degradation within a span of scales, from the full cell down to atoms, a number of techniques are considered. Electrochemical methods like cyclic voltammetry and current interruption techniques can evaluate changes in electrochemical performance and provide insights into individual degradation contributions at both the cell and electrode levels. Material analysis tools include techniques such as Scanning Electron Microscopy and

Energy Dispersive X-ray Spectroscopy give information on electrode-level and particle level. Inductively Coupled Plasma Spectroscopy and X-ray Diffraction provide average or long-range information on the sample and are useful to understand both elemental and structural changes. Transmission electron microscopy, X-ray absorption spectroscopy, Extended X-ray Absorption Fine Structure, Near Edge X-ray Absorption Fine Structure and Resonant Inelastic X-ray Scattering are the techniques that provide information on the atom level. A goal of this thesis is to evaluate if a combination of these multiscale methods can better aid in understanding degradation by directly examining the deteriorated material to identify and understand the underlying ageing mechanisms.

# 3. Experimental Methods: tools for LIBs diagnostics

The goal of this chapter is to give a brief introduction to the techniques that are mentioned in the chapter "4. Summary of the key results and discussion" with a stronger focus on the material characterization. This chapter describes key methods that were used by the author. To gain more insights on battery characterization methods, the following review articles are recommended: synchrotron characterization methods,[72–74] in-house characterization methods,[75] disassembly and electrochemical methods.[76,77]

## 3.1 Cells used in the study

In the current work, two types of cells were studied: cylindrical cells extracted from a battery pack of the Tesla 3 long Range 2018 (used in **Paper I**, **Paper III**, **Paper IV**, **Paper V**, **Paper VI**, and **Paper VII**) and prismatic cells (used in Paper II). The cells are presented in Figure 7 (a) and (b) correspondingly. Both cells have Ni-rich layered oxide as positive electrode active material ($LiNi_{1-x-y}Co_xAl_yO_2$ in cylindrical cells and $LiNi_{1-x-y}Co_xMn_yO_2$ in the prismatic cells) and graphite-based negative electrode (Si-graphite blend in cylindrical cells and pure graphite in prismatic cell).

The commercial cells were aged in different ranges of State of Charge (SoC) and temperatures. This was done to understand how various parameters influence the degradation of the studied cells. The description of the samples is presented in Table 1, where the sample names, types of the cells, together with ageing conditions, and end-of-life (EoL) specifications are presented. The sample names for the cylindrical cells denote the ageing conditions. The temperature of the cycling during ageing is defined by the first letter: R is for 22°C and H is for 45°C. The numbers following the letter correspond to the SoC range cut-off used: 0-50 corresponds to cycling within 0-50% SoC or 2.55 - 3.78 V, 50-100 corresponds to cycling within 50-100% SoC or 3.53 - 4.18 V, and 0-100 corresponds to cycling within 0-100% SoC or 2.55 - 4.18 V. The BoL sample is an exception as it is an unaged cell. The prismatic cell names are self-explanatory.

a

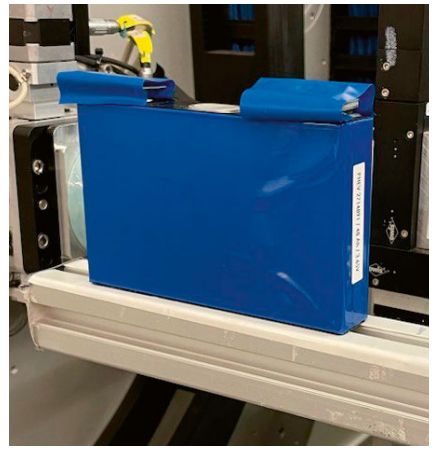

b

Figure 7 – The cylindrical (a) and prismatic (b) cells which were used in the study. The photos are taken during a beamtime in Deutsches Elektronen-Synchrotron Facility (DESY) P02.1 beamline.

Table 1 – Description of the cells used in the study

| Samples names | Electrodes Chemistry | Ageing temperature | Ageing SoC | FCE | SoH |
|---|---|---|---|---|---|
| °BoL/Fresh* | NCA/Si-Gr | - | - | - | 100% |
| °R0-50 | NCA/Si-Gr | 22°C | 0-50% | 800 | 73.35% |
| °R50-100 | NCA/Si-Gr | 22°C | 50-100% | 2570 | 79.41% |
| °R0-100 | NCA/Si-Gr | 22°C | 0-100% | 900 | 73.47% |
| °H0-50/AgedL* | NCA/Si-Gr | 45°C | 0-50% | 950 | 75.99% |
| °H50-100 | NCA/Si-Gr | 45°C | 50-100% | 1950 | 75.05% |
| °H0-100/AgedH* | NCA/Si-Gr | 45°C | 0-100% | 1050 | 72.35% |
| ▫Prismatic Fresh | NMC811/Gr | - | - | - | 100% |
| ▫Prismatic Aged | NMC811/Gr | 33°C | 5-95% | 2891 | 57% |

° - cylindrical cell; ▫ - prismatic cell; * - variations in sample naming in some of the papers

The presented cells have duplicates, which is not specified here. The results from additional datasets are represented in error bars.

## 3.2 Experimental conditions

Understanding degradation in LIBs provides important insights into how to improve materials further and extend the battery life. The diagnostic of LIBs can be done during different stages of a battery life: by monitoring its

performance during operation as well as performing post-mortem characterisation. In the current studies, various battery experimental conditions were used.

*In situ*, *ex situ* and *operando* concepts are used to reflect the state of the analysed system (Figure 8 reproduced from Ref.[78]). *Operando* experiments are considered the most representative of the battery operation as the device should operate normally during the measurements. *In situ* analysis requires the system to be as it is and partially operate, however, the system is typically in a stationary state. *Ex situ* measurements typically involve the extraction of the compounds from the system. The *post mortem* characterization can be destructive and non-destructive. The destructive *post mortem* characterization can also be called *ex situ*. The problem with most of the destructive characterizations is the introduction of the artefacts, which can alter the derived conclusion. Understanding the limitations of the applied methods and evaluating possible impacts on the conclusions is an important part of the results discussion.

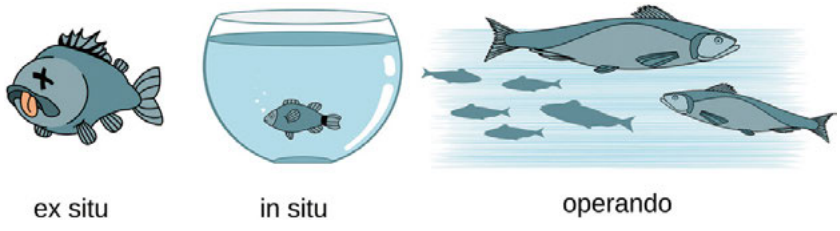


Figure 8 – Analogy of analysing energy material at different states. Reproduced from Ref.[78] with permission from Wiley. ©2021 John Wiley&Sons, Inc.

## 3.3 Cell disassembly and electrode preparation

For post-mortem characterization, electrodes are extracted from the cell. It's crucial to ensure that the cell is discharged before disassembly to minimize risks. The process of opening the cell takes place in an argon-filled glovebox and involves several steps. Initially, the safety valve is opened or the casing is punctured. If feasible, the electrolyte is drained from the cell, following which the cell is left overnight under a vacuum to evaporate any remaining electrolyte, thereby reducing the risk of a short circuit during the cell opening. Subsequently, the casing is carefully removed from the cell. The electrodes are then unrolled and visually assessed.

In this work, the extracted electrodes are divided into segments to ensure that Regions of Interest (ROI) can be compared across different cells. The electrodes are further stored in pre-dried, plastic bags with labels indicating the segment's numbers and their position in the cell (the positive terminal, negative terminal and the neighbouring segments). For additional electrochemical testing, part of the coating is mechanically removed. The absence of

the effect induced by electrode handling is verified using Scanning Electron Microscopy in conjunction with ion polishing (further details on the sample preparation are specified later).

## 3.4 Electrochemical methods for LIBs ageing characterization

The electrochemical characterization of the LIBs starts by analysing their performance. The effects of the calendar and cycle ageing are generally differentiated. For calendar ageing, a set of cells can be stored on a shelf (typically under various temperature and SoC conditions) and their performance is analysed periodically as a function of time.[79] Cycle ageing is usually analysed at different temperatures, cut-off voltage, current rate and other factors of interest as a function of the performed cycles. It is important to note that the conditions of the battery performance in EV and battery testing often have discrepancies as conditions are hard to be repeated. For the in-house battery testing, a number of standard protocols can be applied depending on the aim of the experiment. For the evaluation of the battery capacity retention, reference performance tests are done and the capacity decay is reflected as a capacity retention *vs* number of full cycle equivalents (relation between total throughput to nominal capacity of the cell).

The cycling curve of a battery material is the convolution of the electrochemical responses of the electrodes and side reactions, which also take place in the electrochemical system. The lithium intercalation is a Faradaic process, which means it is associated with redox reactions (charge transfer reactions) processes. Non-Faradaic process involves the formation of the electrical double layers that generate current.[80]

The absence of a reference electrode in commercial cells, capable of deconvoluting the contributions of the positive and negative electrodes, complicates the electrochemical assessment during the ageing analysis. Additionally, the degradation inhomogeneity cannot always be assessed using standard methods on commercial cells.

The extracted electrodes can be further analysed using either two-electrode or three-electrode setups. The two-electrode setup could be a full-cell or a half-cell. A half-cell includes a working electrode with lithium serving as a counter electrode, that assumes an "infinite" lithium inventory. In this setup, the working electrode is studied against a lithium reference, allowing for the assessment of such issues as the loss of active material. Both the three-electrode cell measurements and half-cell measurements, enable the deconvolution of degradation contributions and facilitate more precise diagnostic evaluations of the cell with better parameter control.

The extracted electrodes can be assembled into a pouch cells, coin cells, or a specially designed operando cell. For assembling a pouch cell, which were mostly used in this study, a working electrode is punched out, positioned, and

then sealed under a vacuum along with a lithium chip, a separator (typically PP/PE), and an electrolyte (LP40, 1 M LiPF6 in 1:1 EC:DEC).

The electrochemical evaluation methods in this thesis include cyclic voltammetry, galvanostatic intermittent titration technique, incremental capacity analysis, and electrochemical impedance spectroscopy. Both full and half-cell measurements were also examined using Incremental Capacity Analysis (ICA) and Differential Voltage Analysis (DVA), providing a broad spectrum of analytical lenses to better understand the electrochemical behaviours and degradation mechanisms within the cells.

### 3.4.1 Intermittent Current Interruption

Intermittent Current Interruption (ICI) is a relatively new test protocol that is used to evaluate the resistance of the batteries.[81] The method includes galvanostatic cycling and short current pauses. The typical time of the constant current step is five minutes and the rest can vary from 2 to 10 s, and these can be varied significantly depending on the needs and properties of the cell under investigation. The potential response is recorded with significantly higher frequency during the current pauses. The technique and the data analysis method were originally developed by Lacey *et al.* and derived resistances are valid for any battery cell where the potential response is diffusion-controlled within an appropriate time window after the current interruption.[81–83]

The ICI method can be used to characterise energy loss processes broadly into time-independent and time-dependent quantities during the cell performance. The parameters are derived per each current pulse. During a step, first, an instant drop of voltage governed by the internal resistance (termed $R$) takes place, which typically includes contributions such as ionic and electronic resistances and charge transfer resistances in the electrode materials. The second part is the voltage relaxation driven by mass transport (diffusive) processes. A diffusion resistance coefficient, $k$, can be derived from parameters extracted from the voltage relaxation during the current interruption where $d\Delta E$ is the potential change during the current interruption step and t is the time of the potential change:[84]

$$k = -\frac{1}{I} \cdot \frac{d\Delta E}{dt^{0.5}} \tag{3.1}$$

Traditionally, the diffusion parameters are analysed using Electrochemical Impedance Spectroscopy (EIS) or Galvanostatic Intermittent Titration Technique. The k parameter is related to the Warburg parameter σ which is used in EIS analysis:[84]

$$k = \sqrt{\frac{8}{\pi}}\sigma \tag{3.2}$$

GITT and EIS are time consuming and EIS requires a special equipment. ICI does not significantly extend the experiment time and was shown to successfully reflect the diffusion values.

## 3.5 Material analysis methods for studying LIBs degradation

Battery components include a wide range of materials with a number of chemical elements and varying properties. As described before, battery materials contain light and heavy elements, solids and liquids, crystalline and amorphous materials. The analysis of battery components is therefore challenging yet exciting. The selection of an appropriate technique necessitates a thorough evaluation of the technique capabilities and limitations. The choice of technique can significantly impact the quality and accuracy of the acquired data and, consequently, results.

In addition to that, the ability to perform *in situ* or *operando* analyses is beneficial for studying battery materials under realistic operational conditions. Techniques with *operando* capabilities provide dynamic insights into the materials as they operate, facilitating a more accurate understanding of their behaviour and degradation mechanisms.

The work conducted within the current thesis framework was mostly focused on the analysis of the crystalline layered transition metal oxides which involved the significant presence of diffraction-based technique. The priority of studies was given to *operando* methods. However, some of the techniques have limitations to that. In such case, the closest approximation that allowed evaluation of the material state in conditions closest to its standard operation compromised with data collection quality was used.

### 3.5.1 X-Ray diffraction

X-ray diffraction (XRD) is a technique used to study the crystal structure and composition of materials.[85] The active electrode materials studied in this thesis are crystalline, which means that their crystallographic structure complies with rules of symmetry and periodicity. The interaction of an incoming X-ray beam with such material occurs according to Bragg's law (3.3) where n is an integer ($n \geq 1$), $\lambda$ is the incoming radiation wavelength, $d_{hkl}$ is an interplanar spacing with *hkl* being Miller indices denoting index of a plane, and $\theta$ is the scattering angle:

$$n\lambda = 2d_{hkl}sin\theta \tag{3.3}$$

As a result of elastic interaction (no energy exchange), diffraction patterns are produced where the diffracted x-rays can be detected as intensity peaks due to the constructive interference. These diffraction patterns can then be used to determine the crystal structure and composition of the material.[86]

XRD is a powerful tool for analysing battery materials as it can be used *in situ*, *ex situ* and *operando* on crystalline materials in the battery. It is limited with respect to the light elements, which is a significant limitation in the case of Li-ion battery electrodes, as it cannot directly show lithium.

In the current thesis, the studies of the powder diffraction were done in-house using transmission mode on a STOE Stadi P diffractometer, utilizing

both Mo Kα radiation (**Paper I, IV**). In **Paper I** the samples were extracted from electrodes mechanically, homogenized using mortar and pestle and sealed in quartz capillaries in an Ar-filled glovebox in order to avoid degradation due to air exposure, which is known to be harmful for Ni-rich electrodes.[87]

In **Paper IV**, the same diffractometer was used, but instead of placing electrodes in the capillary, a pouch cell was placed in a holder and analysed during its cycling *operando*. The presence of conductive carbon and binder does not interfere with the measurements as those compounds are not crystalline and do not increase the background significantly.

In **Paper II**, XRD was employed as a technique for Diffraction Radiography. The cells were examined in their intact state, as the intensity and transmission of synchrotron radiation are adequate for studying the commercial cells directly. Figure 7 displays both cells positioned on the sample stage at beamline P02.1 DESY, Germany. Diffraction radiography is an imaging method utilizing X-rays, where a raster scan is performed over the sample, and the resulting diffraction patterns are analysed. This technique facilitates the analysis of the crystallographic structure, allowing for spatial resolution of any changes in the material under study.

Various approaches to XRD data treatment were also used in the study. For instance, classic Rietveld refinement was conducted on the operando data in batch modes using commercial software such as Topas,[88] and FullProf.[89] Notably, batch refinement mode typically necessitates a gradual alteration of the parameters, which is not always feasible with raster scans. Therefore, careful analysis and regrouping of the data are essential to ensure smooth refinement processes.

Another type of XRD study that was done in this thesis is *in situ* nano-resolved Scanning X-ray Diffraction Microscopy (**Paper III**). The photograph of the setup is demonstrated in Figure 9. The experiment was done using pouch cells with electrodes, extracted from the EV batteries. For that, a thinned electrode is used to ensure a single layer of the secondary particles. The data is typically processed and calibrated using the $LaB_6$ standard powder reference and is processed to capture the gradient over a secondary particle. For example, conversion of the data to polar coordinates with the centre inside a particle can facilitate the data interpretation. The scripts for the data processing are usually developed by the user in Python.

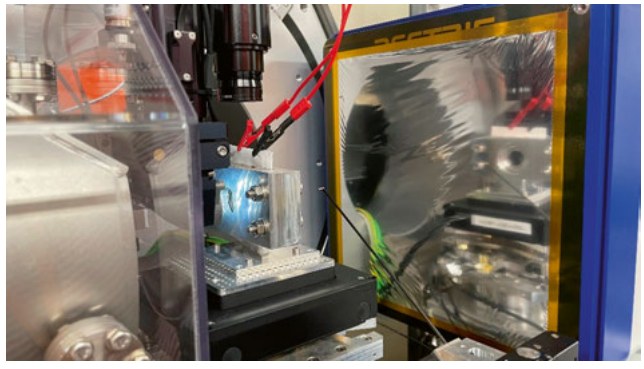

Figure 9 – Setup at NanoMAX beamline, MAXIV, Sweden. From **Paper III**.

### 3.5.2 Scanning electron microscopy

Scanning electron microscopy (SEM) is an analytical technique used to study the surface morphology and composition of materials. An electron beam interacts with the sample. The focused electron beam performs raster scans over the sample mainly interacting with its surface. As a result, secondary electrons, backscattered electrons and X-rays are produced. The penetration depth can be varied using different acceleration voltages, which changes the energy of the incoming electron beam. For example, higher beam has higher probing depth and, therefore, its application allows to obtain the information on material.

In the current work, two SEM-based methods are used:

1. **Secondary electrons scanning electron microscopy** – the incoming electrons interact inelastically (energy exchange is present) with electrons of the studied material. The contrast of the image reflects material topology.

2. **Energy-dispersive X-ray Spectroscopy (EDX)** – the incoming electron beam generates X-rays from the sample. The X-ray energy is specific to various elements and excitation levels (*K, L, etc*). This technique can be used to study elemental distribution inside the materials.

SEM has a wide range of applications for battery research: it can perform the characterization of solid crystalline and amorphous materials. Modern SEM equipment has air-tight transfer chambers, which allows to keep the sensitive parts from interaction with ambient air. In-house SEMs usually allow to study only the surface of the samples, however, by using various sample preparation methods (*i.e.* cross-section polishing) depth-resolved information can be obtained.[90]

In **Paper I** and **III** sample preparation using ion-polishing was conducted. For that, the sample was installed on a holder using carbon tape. It ensured electric conductivity for the following measurements. The voltage and time were selected based on the electrode material and coating thickness.

### 3.5.3 Inductively coupled plasma optical emission spectroscopy

Inductively Coupled Plasma Optical Emission Spectroscopy (ICP-OES) is an analytical technique used to study the elemental composition by measuring the light emitted from excited atoms within the sample. In ICP-OES, a sample is introduced into a plasma generated by an inductively coupled radiofrequency generator. The energy imparted by the plasma excites the atoms within the sample, leading them to emit light upon decay. The emitted light is processed by a spectrometer, which segregates the light into its constituent wavelengths and detects the light emitted by each element. The concentrations of the elements are typically deduced using calibration solutions.

Sample preparation is a pivotal aspect of ICP-OES, particularly in the analysis of battery materials where different components require tailored preparation procedures. In the present study, analyses were conducted on active material powders extracted from electrodes. To facilitate this, the material was initially detached from the current collector, followed by a filtration process to remove inactive compounds, achieved by dissolving the material in a mixture of N-Methyl-2-pyrrolidone (NMP) and ethanol. Subsequently, the mixture was digested using acids, and any residual carbon was eliminated through filtration. The analysed amounts of elements are typically normalized to the electrode areas or electrode material mass.

### 3.4.4 X-ray Absorption Spectroscopy

X-ray Absorption Spectroscopy (XAS) is an X-ray-based technique that facilitates the examination of the chemical state and local environment of atoms within materials. The procedure entails tuning the beam energy over a specific absorption edge, which is characteristic of particular atoms and types of electron excitations (edges). Generally, three distinct regions are observed in XAS spectra: the pre-edge, rising edge, and extended region. The pre-edge signal reveals the local coordination of the atom's surroundings, while the rising edge is influenced by the chemical state of the material. An analysis of energies within this part is referred to as X-ray Absorption Near Edge Structure (XANES). The extended range is shaped by the constructive and destructive interferences between the ejected photoelectron and neighbouring atoms. Extended X-Ray Absorption Fine Structure (EXAFS) aids in determining the distances and coordination numbers of the atoms within the material.[91]

The **Paper V** included EXAFS *ex-situ post-mortem* characterization. For that purpose, the electrodes were assembled into half-cells and delithiated. The samples were further packed in air free atmosphere and placed on a sample holder using kapton tape.

In this thesis, XANES was used *operando* during the cycling of material in the pouch cell, offering real-time insights into the evolving structural and chemical dynamics. An example of the *operando* setup is presented in Figure

10. The data collection included a randomized electrode scanning in order to limit the beam damage, which is a highly relevant issue in synchrotron-based operando battery characterization studies.[92]

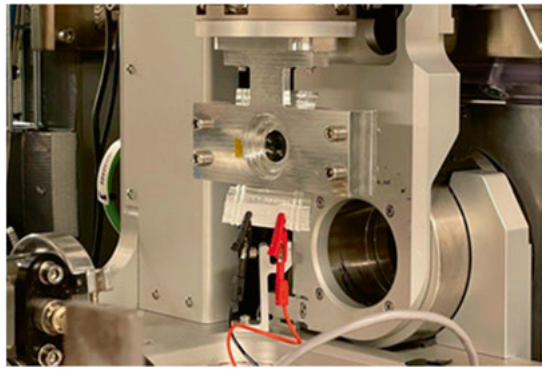

Figure 10 – Pouch cell in the operando holder installed onto sample holder during beamtime on Balder beamline, MAXIV, Sweden. From **Paper VI**.

### 3.4.5 Resonant X-ray Inelastic Scattering

Resonant Inelastic X-ray Scattering (RIXS) is an experimental technique employed to analyse momentum, transferred energy, and polarization. Like XAS, RIXS is element-specific, with the energy of the incoming photon being specific to the element and edge in question.

The RIXS process begins with an incoming photon exciting an electron from the ground state. This excitation promotes an electron from a filled core shell to the valence shell, while another electron from the valence shell descends to fill the core hole. This transition is accompanied by the emission of an outgoing photon, the energy of which is measured using a spectrometer. The energy difference between the incoming and outgoing photons corresponds to the energy of excitations within the sample.[93]

**Papers V** and **VII** delineate RIXS studies conducted on NCA cathodes. For these experiments, the materials underwent charging/discharging in half-cells, after which the electrodes were extracted and positioned on a sample holder.

# 4. Summary of key results and discussion

This chapter consolidates key findings from **Paper I** to **Paper VII**, shedding light on the ageing processes within commercial cells designed for electric road vehicles, with a special emphasis on the positive electrode. The findings presented in **Paper I** serve as a foundation of the thesis work and cover the extensive degradation of commercial cells from the extended matrix of varying operation conditions. This thesis spans various scales of investigation, starting from the full cell analysis and delving into the deconvolution of single process contributions into battery ageing. **Papers II** and **III** explore the heterogeneity of cell degradation, examining it both at the macro level of the prismatic cell and within the secondary particle level *in situ*, respectively. **Paper IV** focuses on the examination of structural changes within Ni-rich material and its relationship to dynamic processes occurring within the material during operation beyond the stability region. **Paper V** and **Paper VI** transition to an atomistic level, exploring respectively the role of the redox centres in the cathode materials as well as the role of oxygen in depth *ex situ* and *operando*. The papers contextualize the findings within the framework of ageing. **Paper VII** extends the exploration to degradation products formed during cell cycling and follows the evolution of the hydroxide group in the cathode material upon ageing. Figure 11 illustrates the connection between the papers listed above.

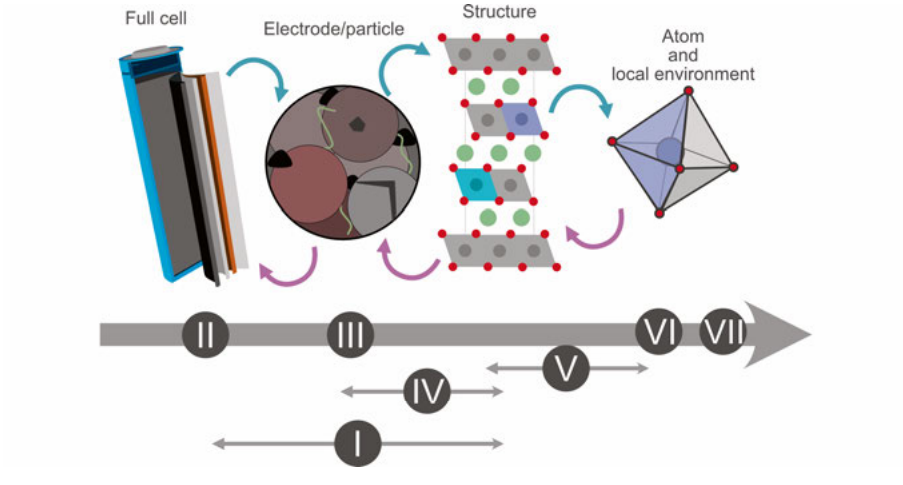


Figure 11 – Overview of the papers presented as a function of the scale of the studied processes.

In the current chapter, the results are organized in descending order of the length scale: beginning with macro-level studies on the full cell, narrowing down to the electrode level, then to the structure level, and finally towards the atomistic level, with a focus on addressing fundamental questions important for ageing. Extensive cross-references between papers are employed in this summary as the thesis aims to correlate changes across scales and understand the underlying causes of performance decay in the cells.

## 4.1 Cycle-life ageing of cells for electric cars

The batteries in electric cars experience challenging operation conditions[94] that provokes various ageing mechanisms and further lead to a high level of uncertainty in predicting their long-term performance.[95] This highlights the necessity of examining commercially relevant systems. The commercial cells used in this thesis were electrochemically cycled and studied in various conditions: different SoC ranges, temperatures, and cell formats. Capacity retention trends are an important indicator of the degradation processes taking place inside the battery.[96] The results of the cells' performances are presented in Figure 12 for (a) cylindrical cells (**Paper I**) and (b) prismatic cells (**Paper II**). The studied cells showed two different types of capacity decline: sublinear degradation (Figure 12 (a)) and superlinear degradation (Figure 12 (b)). The first trend is considered typical for the cases where the degradation is driven by side reactions such as SEI growth. This type of degradation was found in all cells presented in **Paper I** with significant ageing of $SiO_x$ component. The second type of the degradation is typical for cells that decline due to Li plating. A more detailed study on Li plating was done on the cell and the Li plating presence was confirmed.[97]

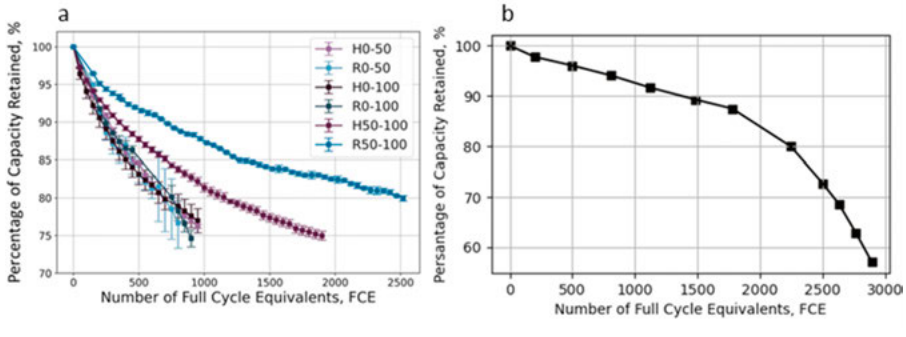


Figure 12 – The capacity retention of two systems: cylindrical cells (a) and prismatic cell (b) presented as a percentage of Capacity retained versus a number of Full cycle equivalents. From **Papers I** and **II**.

The cylindrical cells were examined under various conditions (details on the EoL status of the cell can be found in Table 1). Degradation was found to be similar for all cells cycled down to 0% SoC, suggesting that processes at low potentials are dominant and not significantly enhanced by elevated temperature when cycling under such conditions. Conversely, the cells cycled at 50-100% SoC exhibited significant variation from other conditions and were found to be temperature-dependent.

## 4.2 Ageing heterogeneity

The degradation of batteries is known to be inhomogeneous. The sources are multiple: from inconsistencies introduced during manufacturing to differences in materials' response during battery functioning. The heterogeneity of the battery is also a multiscale process. The differences in local SoC, for example, can be resolved within the battery in-plane or thickness geometry,[97–100] electrode scale,[101–104] and secondary particle level.[105–107]

### 4.2.1 In-cell heterogeneity

In this work, two types of cells were investigated: cylindrical and prismatic. For the prismatic cell, the focus was on in-plane heterogeneity (**Paper II**). The cells were analysed after ageing using X-ray radiography (Figure 13). The XRD mapping was carried out in one plane of a prismatic cell and experimental setup is presented in Figure 7 (b). In the collected patterns, peak assessment was conducted and the position of the diffraction peaks *hkl = 300* of NMC811 and *hkl = 002* of $Li_xC$ (lithiated graphite) was analysed in comparison to positions of the respective diffraction peaks in the fresh cell. Notably, such study averages the information within the thickness of the cell. The *(300)* reflection, originating from *hkl = 300* plane of the NMC811 active material, was used for heterogeneity evaluation of the positive electrode as it reflects changes in *c* lattice parameter of the structure. Notably, the *(300)* reflection in Ni-rich layered oxide chemistries from $R\bar{3}m$ symmetry group is sensitive to the Li content in the structure.[42] The change of the *(300)* reflection is not linear within the whole electrode potential span. The c lattice parameter, first semi-linearly increases upon NMC811 delithiation until reaching ~4.0 V. After that, the c lattice parameter abruptly decreases. Figure 13 (a) displays the heatmap of the positive electrode *(300)* reflection shift. Interestingly, the data points indicate that the entire NMC811 material in the aged cell has a lower Li content compared to the fresh cell. This happens when some of the Li-ions are lost due to the various parasitic reactions and cannot be intercalated back into the positive electrode. This indicates that there is an increased LLI and explains part of the capacity loss. Moreover, the material's state (degree of delithiation) is visibly uneven across the cell. Two "hot spots" with higher

differences Δq are identified: the spot labelled “3” indicates the area of the cell where the lattice parameter has the largest negative shift relative to the "fresh" value, implying lower degree of lithiation in the location. This suggests that the material in this area of the electrode has the most significant increase in the c lattice parameter. This area is located near the positive tab of the electrode and it is likely that the lower degree of lithiation is linked to the current distribution gradient in this region. The second spot is labelled “1” and shows the highest lithiation state across the aged cell, while lithiation state is still lower than in the fresh sample. This indicates the region where the positive electrode has the lowest degradation.

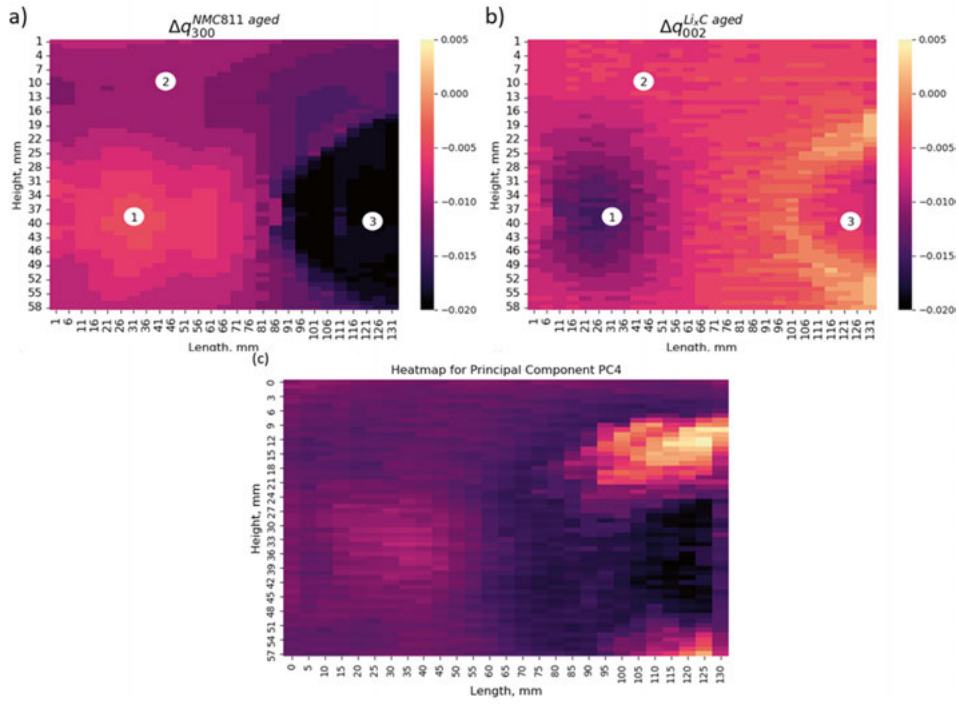


Figure 13 – Heatmap of prismatic cell radiography: (a) reflection shift corresponding to (300) reflection of the NMC811, (b) reflection shift corresponding to graphite. The colour scale shows Δq values and follows the same scale for both figures. Heatmap of a positive electrode phase which operates independently form the graphite (c). The colour scale represents a relative presence of the phase. From **Paper II**.

Figure 13 (b) presents a heatmap depicting the variance in the graphite reflection within the prismatic cell. The image is displayed in a similar manner as the positive electrode's reflection. Unlike the positive electrode, a portion of the graphite remains in the same state as in the fresh electrode, suggesting that the positive electrode may be more significantly impacted by ageing in this region. The distribution of reflection heterogeneity in the negative electrode

somewhat mirrors that in the positive electrode, albeit with contrasting trends. The hotspots are similarly located, yet exhibit opposing trends: in area "1" the material displays the largest deviation from the unaged material, indicating the highest lithium content within the cell.

Figure 13 (c) presents a distribution of a phase that is part of the positive electrode opposite to the lithium plating region. This region is found to still be electrochemically active *versus* the lithium known to be plated on the negative electrode. This material is also located around the region "3", close to the side with the positive tab, confirming that this part of the cell is significantly more vulnerable towards accelerated degradation. An improved cell and pack design are required to mitigate gradients in the cell ageing for longer and safer operating life.

Investigating pronounced heterogeneities is challenging as the deviations in material degradation are observed both in-plane of the cell and along its length. Figure 14 displays photographs taken during the teardown of the cell characterized using XRD radiography. The degradation within the cell is so substantial that visual examination alone can trace the deterioration. However, for a more nuanced understanding, 3D analytical methods are essential, though they may not always be feasible for large-format cells.

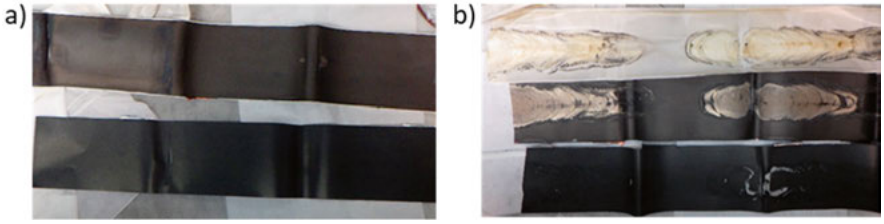


Figure 14 – Photographs from the Prismatic Aged cell teardown: (a) shows the beginning of the jellyroll with the negative electrode at the top and the positive at the bottom; (b) the middle of the jellyroll with separator at the top of the photograph, the negative electrode is in the middle and the positive electrode is displayed at the bottom. On both photographs the negative electrode is displayed upside down to depict the facing sides of the positive and the negative electrode. From **Paper II**.

Heterogeneity within the cell geometry of a cylindrical cell was also investigated (**Paper I**). For that purpose, the electrodes extracted from the cell were divided into segments, where Region 1 was the closest to the casing of the cylindrical cell and Region 6 was at the cell core. The central region was also split into 3 segments: upper (at the positive terminal), middle, and lower (at the negative terminal). The evaluation of the capacity loss in these segments has shown that the positive electrode was preserved closer to the core within the cell roll and closer to the negative electrode within the cell height. The capacity loss variation across the measured regions was stronger at the positive electrode. However, the strongest damage was found in the centre of the

Region 4, see Figure 15. In the negative electrode, the capacity loss was mostly found to be stronger next to the negative terminal.

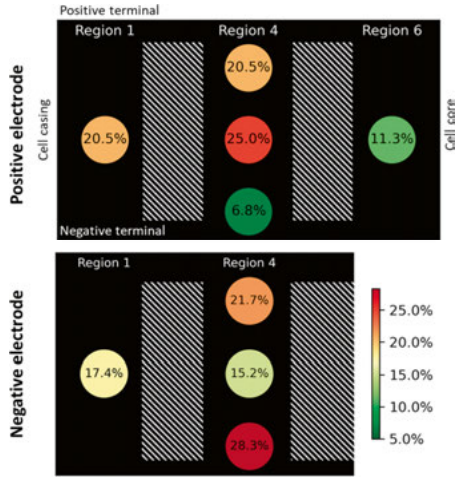


Figure 15 – A degradation heterogeneity within the roll of the cylindrical cell accessed electrochemically. From **Paper I**.

Combining the results presented for the different commercial cells it is shown that heterogeneity is an important aspect of cell ageing. Notably, the spatial distribution trend of the degradation heterogeneity significantly varies between two cell geometries. This highlights that the heterogeneity in degradation is strongly influenced by cell design, and optimization of this should yield more long-term stable batteries.

### 4.2.2 In-particle heterogeneity

The heterogeneity within a secondary particle from an electrode of the cylindrical cell cycled at 40°C and 0-100% SoC (H0-100) was studied using *in situ* nano-resolved Scanning X-ray Diffraction Microscopy in **Paper III**. The choice of cell was motivated by highest ageing of the positive electrode that was presented in **Paper I**. The probed particles are displayed in Figure 16 (a), while the NCA reflection *(300) q* collected over the circled particle is displayed as a function of the particle radius *r* in Figure 16 (b - i). The *(300)* reflection intensity is shown as a function of *q*. The four lithiation states are demonstrated in the Figure 16: 3.60 (b, c), 3.85 (d, e), 4.15 (f, g), and 4.33 V (h, i). The change of the lithiation state of the material within the particle shows high heterogeneity at the beginning of the delithiation (Figure 16 (b, c)). This is might be a cause of the $Li^+$ diffusion resistance increase shown in the sample in **Paper I**. During this *in situ* study, where the cycling includes potential hold during mapping collection, the heterogeneity is decreasing and

the particle performs further cycling with significantly higher homogeneity during cycling.

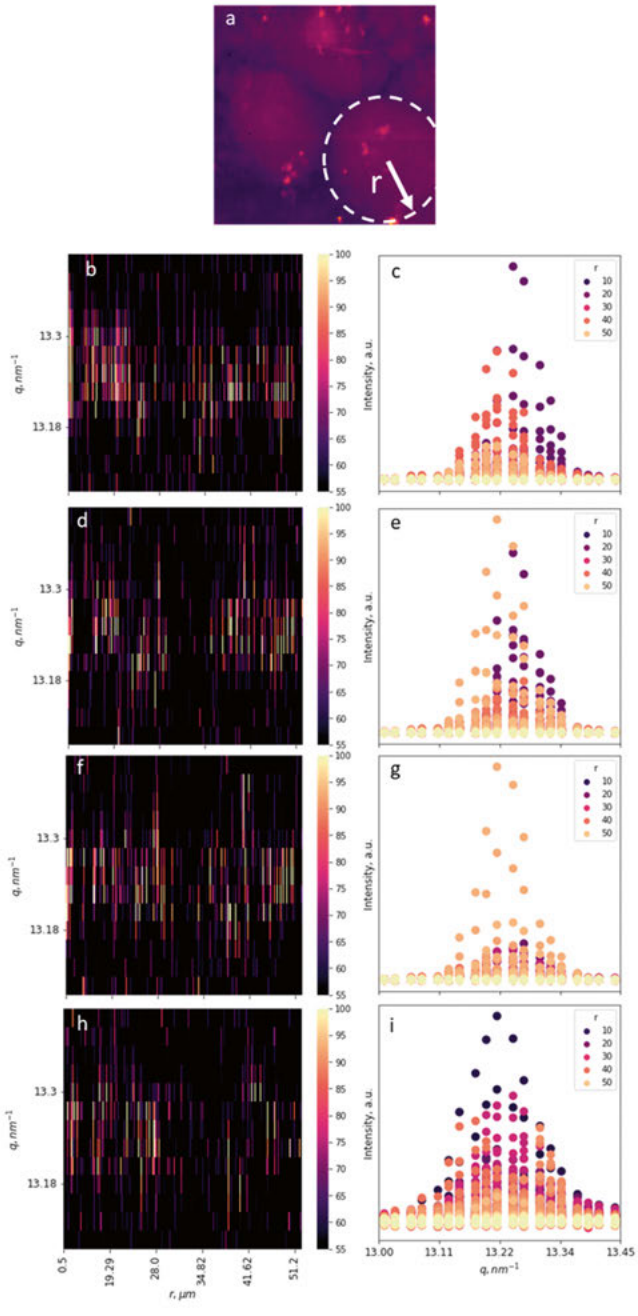


Figure 16 – The distribution of the diffraction reflections as a function of position inside the particle and the potential of the electrode vs $Li/Li^+$: 3.60 V (b, c), 3.85 V (d, e), 4.05 V (f, g), 4.33 V (h, i). From **Paper III**.

## 4.3 Evaluation of individual electrode contributions

In order to standardize the evaluation of ageing processes within LIB cells, degradation modes are introduced. The evaluation of these degradation modes is typically conducted by analysing the electrochemical performance of the cells under study. While the alterations in the positive and negative electrodes upon ageing are interconnected, these changes are distinct and specific for the electrode chemistry and operational conditions. **Paper I** evaluates the degradation in both the positive and negative electrodes, respectively, analysing and connecting the trends to the electrochemical performance of the full cell. The capacity loss, and changes in the $Li^+$ diffusion resistance coefficient in both electrodes are illustrated in Figure 17 (a) and (b) respectively.

Figure 17 (a) compares capacity loss measured in positive and negative electrodes after ageing cylindrical cells under various conditions. Notably, the degradation of all cells cycled at room temperature is dominated by capacity loss on the negative electrode. The same conclusion can be drawn for the high-temperature cell cycled at a low SoC range. However, at higher temperatures cells that were reaching 100% SoC during their charge had a degradation that was dominated by the positive electrode capacity loss. High Ni content is sensitive to operation in higher delithiation states,[108] which supports the observed trends. However, the presence of $SiO_x$ complicates the ageing predictions as its instability is known to be linked to a strong degradation taking place in the particles: $SiO_x$ particle disconnection as a result of the volume change inside the material upon lithiation and delithiation as well as surface reactivity.[42]

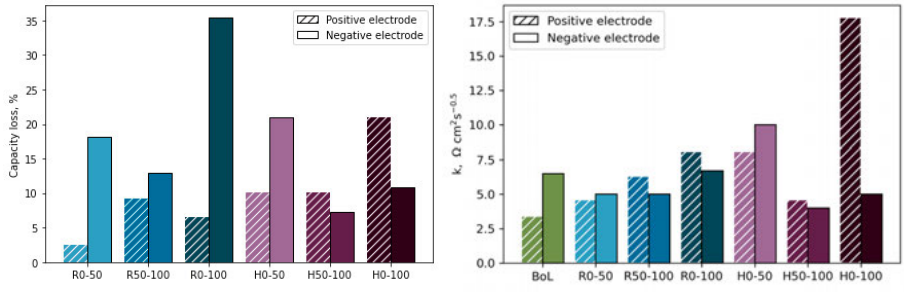


Figure 17 – The results of testing by varying temperature and SoC cycling conditions of the cylindrical cells is presented in the figure. The positive and negative electrode capacities are studied in half-cell configuration (a). The $Li^+$ diffusion resistance coefficient measured for the positive and negative electrodes studied at various conditions (b). From **Paper I**.

Figure 17 (b) shows $Li^+$ diffusion resistance coefficient values in both positive and negative electrodes. The negative electrodes show a decrease rather than increase in almost all cases, which can be caused by decrease in the tortuosity

in graphite because it is prone to exfoliation during the battery operation.[59] The same decrease can happen in the case of $SiO_x$, the observations in morphology indicated increased porosity upon ageing of the particle, which also will be shown later in this thesis. In the positive electrodes, the trend is the opposite, demonstrating an increase in $Li^+$ diffusion coefficient for all cases. The strongest increase in Li-diffusion resistance coefficient is observed in H0-100 sample. The heterogeneity studied in the sample in **Paper II** partially shows an inhomogeneous distribution in SOC within the particle, which in turn is likely an effect of an increase in $Li^+$ diffusion resistance coefficient due to ageing.

## 4.2 Ni-rich positive electrode degradation mechanisms

### 4.2.1 Morphological changes

Ni-rich materials are well-known for their susceptibility to particle cracking.[42,46,58,59,109] Several key factors should be considered when addressing the issue of particle cracking in Ni-rich materials: (i) it's crucial to distinguish between the stresses introduced into the material during synthesis and those developed during ageing, and (ii) the occurrence of particle cracking in the material is State of Charge (SoC) dependent, thus comparisons between fresh and aged materials should account for this aspects.[46,110]

The investigation detailed in **Paper IV** illustrates the observations of the fresh (BoL) NCA electrode cross-section at various states of charge, utilizing SEM as shown in Figure 18. The images reveal the development of cracks within the material, which tend to extend further at higher degrees of delithiation. Conversely, the material exhibits reduced particle cracking upon relithiation.

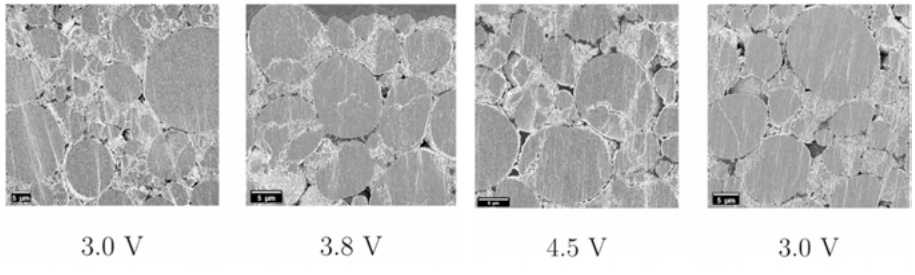


Figure 18 – Comparison of the same material from Fresh cell at different SoCs. From **Paper IV**.

Considering the impact of reversible crack formation on the electrodes, a morphology study was conducted on the positive electrodes of the BoL and H0-100 samples (**Paper I**). The positive electrodes aged in various conditions

were studied in lithiated state and compared to fresh cells, and the SEM images of secondary particles are shown in Figure 19. The electrodes from the Fresh cell show mild particle cracking, which is most probably induced during manufacturing, e.g. stress introduced during synthesis or cracking resulting from calendering.[41] Figure 19 (b) shows the positive electrode aged between 0-100% SoC at 45°C (sample H0-100). In this sample, particles that contain voids in the centre were found. Such voids would have negative effect on the $Li^+$ diffusion in such materials, which was also demonstrated Li-ion resistance increase (H0-100) in **Paper I**. The observed number of such particles clearly containing voids were small, however, the lack of observing such voids in a larger number of particles, can be related to the low statistics of such measurements.

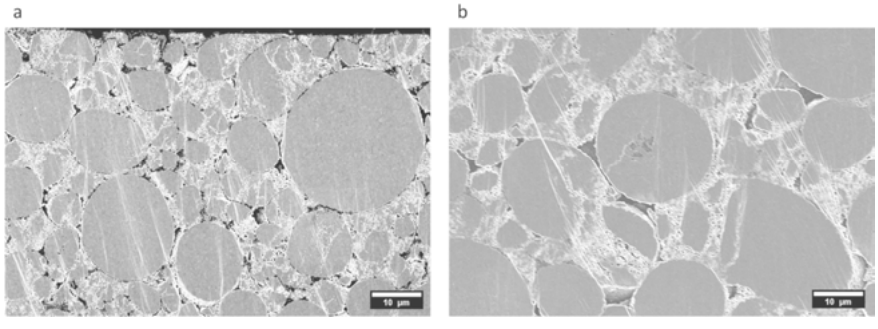


Figure 19 – SEM cross-section images: (a) Fresh sample, (b) H0-100 sample. From **Paper I**.

Interestingly, the primary particle microstructure has undergone significantly more changes, which were registered using TEM. Figure 20 demonstrates differences between fresh (Figure 20 (a)) and aged materials (Figure 20 (b), (c) and (d)). The aged particles show a large number of pores formed upon ageing. In some cases, voids can be found already in synthesised materials both intergranular and in primary particles.[111] However, in the present case, the porosity is clearly formed upon ageing. Interestingly, some of the pores are found to concentrate along the edges of the particles (Figure 20 (c) and (d)). Similar voids have been reported for other cathode chemistries and were connected to oxygen evolution.[112,113] The pores are expected to reduce the stress in the material formed upon delithiation. By existing inside the bulk of the material, they can alter mechanical properties of the bulk and could reduce the cracking of the particles. Apart from tungsten doping, which was found in the material (**Paper I**) and known for the particle cracking mitigation,[114,115] such pores can partially explain lack of particle cracking.

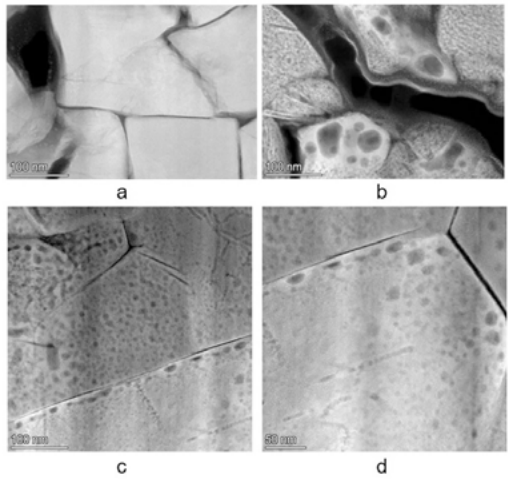


Figure 20 – TEM image of NCA electrodes. From **Paper V**.

### 4.2.2 Transition metal dissolution in Ni-rich transition metal oxide electrodes

The TM dissolution is a phenomenon often blamed for capacity fading and resistance increase in Ni-rich layered oxide-based LIBs. The reason behind this is that TM dissolution has an impact on both the positive and negative electrodes.[61] The origins of the TM dissolution are still debated and include oxygen loss,[62] disproportionation reactions,[116] and acidic leaching.[117] The TMs released from the structure into the electrolyte were found to be later to be deposited in the SEI. The latter results in the growing impedance of the LIB.

In **Paper I,** analysed materials aged under various conditions were studied using ICP-OES. The results show more Ni dissolution was found in the batteries aged at higher SoC compared to the baseline (BoL sample). This agrees with general research, pointing towards a higher degree of the TM dissolution at elevated potentials.[118] Moreover, the study points towards a possible correlation of the TM dissolution to the oxygen evolution, which is also found to be more extensive at higher potentials (shown further in **Paper IV** and **Paper V**).[62] As described before, TM dissolution influences both the positive and negative electrode, however, when comparing the $Li^+$ diffusion resistance coefficient for the positive and the negative electrodes to TM dissolution, no correlation with the amount of TM was found (Figure 17). In case of the positive electrode, instead, other degradation mechanisms might be more detrimental for the electrode performance. In case of the negative electrode, degradation due to TM deposition this may be influenced by the chemistry of the negative electrode, which included both graphite and silicon oxide. Increased TM content in the negative electrode is generally correlated with increased

resistance.[119] However, no distinct correlation between resistance increase and the measured TM dissolution was found in the studied samples. Instead, it is possible that the resistance caused by the deactivation of the $SiO_x$ compound might be dominant in the studied systems and TM-induced resistance might be relatively small in comparison.

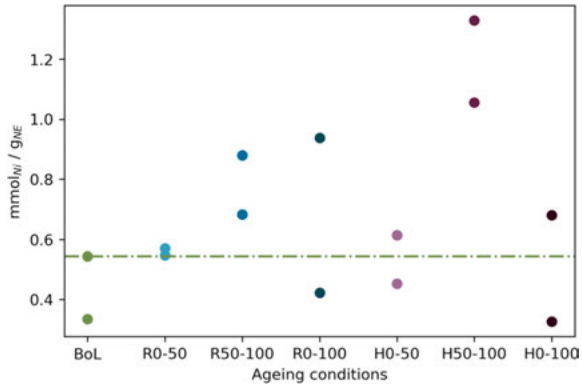


Figure 21 – Ni content detected in negative electrodes of batteries aged within three different SoC ranges and two temperatures. From **Paper I**.

Multiple studies have demonstrated that a Ni depleted region is formed upon ageing in the regions close to the surface of the particle, near the electrolyte.[120] It is shown that such a gradient can enhance materials' properties and increase its stability.[121] On the other hand, if a rock-salt layer is formed in the Ni-depleted region, it can instead result in high resistance to lithium diffusion, thus increasing the overall resistance in the cell.[122] Interestingly, no TM distribution gradient was found in Fresh and H0-100 aged conditions and therefore no connection between TM dissolution and $Li^+$ diffusion resistance coefficient could be made within the frame of the study (**Paper I**).

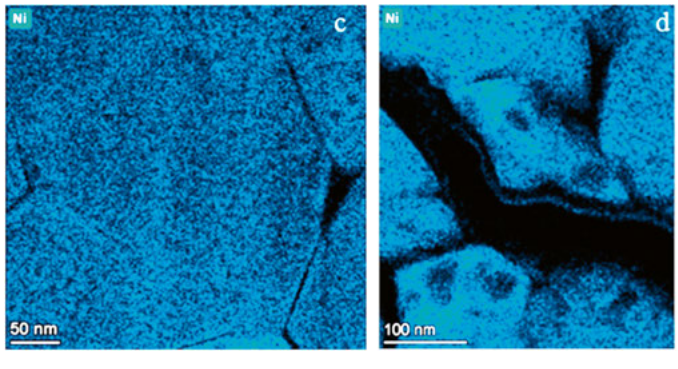


Figure 22 – EDX image of the particles from aged (right) and fresh (left) material showing distribution of Ni across the primary particles cross section. From **Paper I**.

### 4.2.3 Cation mixing

Cation mixing is a common phenomenon observed in Ni-rich layered oxide materials.[42,59,122–125] The term implies the diffusion of Ni atoms into the Li layer and occupation of Li sites. This results in an increase of the lithium diffusion resistance together with a decrease in capacity as the material will lose the sites available for Li-ion accommodation.

There are a number of techniques that detect cation mixing including electron channelling X-ray spectroscopy,[125] and XRD.[123,124] The latter was used in the **Paper I**. The results presented in Table 2 have demonstrate that the highest cation mixing is found in samples cycled until 100% SoC at room temperature and 0-50% SoC cycled at elevated temperatures. In the case of the room temperature, the trend is supported by the increase of the Li diffusion resistance. In the case of the elevated temperature, such a trend was not found, which indicates a different source for significant $Li^+$ diffusion resistance increase.

Table 2 – Crystallographic parameters of studied samples from cylindrical cell. Adapted from **Paper I**.

| Sample | c/a | $I_{003}/I_{104}$ |
|---|---|---|
| BoL | 4.9785 (1) | 1.316 |
| R0-50 | 4.9997 (2) | 1.382 |
| R50-100 | 5.0007 (2) | 1.186 |
| R0-100 | 5.0026 (2) | 1.292 |
| H0-50 | 5.0102 (2) | 1.389 |
| H50-100 | 4.9989 (2) | 1.269 |
| H0-100 | 4.9972 (1) | 1.378 |

### 4.2.4 Oxygen evolution

The gas evolution is a typical problem for Ni-rich layered oxide electrodes.[42,59,62,65,66,126] Particularly, oxygen evolution is monitored through side reaction products CO and $CO_2$.[65] It is proposed that the CO and $CO_2$ originate from electrolyte degradation triggered by reaction with evolved oxygen.[62,127] There is a debate whether the gas formation is driven by reactions on the surface of the particles or within the bulk.[46,62,128] In addition, it is argued that the surface species from side reactions during material synthesis, storage and electrode production are suspected to contribute to the $CO_2$ signal.[65] The amount of evolved gases is also suspected to be decreased due to the cross-talk between positive and negative electrodes as part of the evolved gas will be consumed, which complicates the analysis of the system.[129]

In **Paper IV,** an operando investigation was done to correlate the relationship between changes in the crystal structure, electrochemical properties and gas evolution. The lithiation and delithiation of the full cell were performed

in parallel using operando XRD and OEMS setups, and the results are presented in Figure 23.

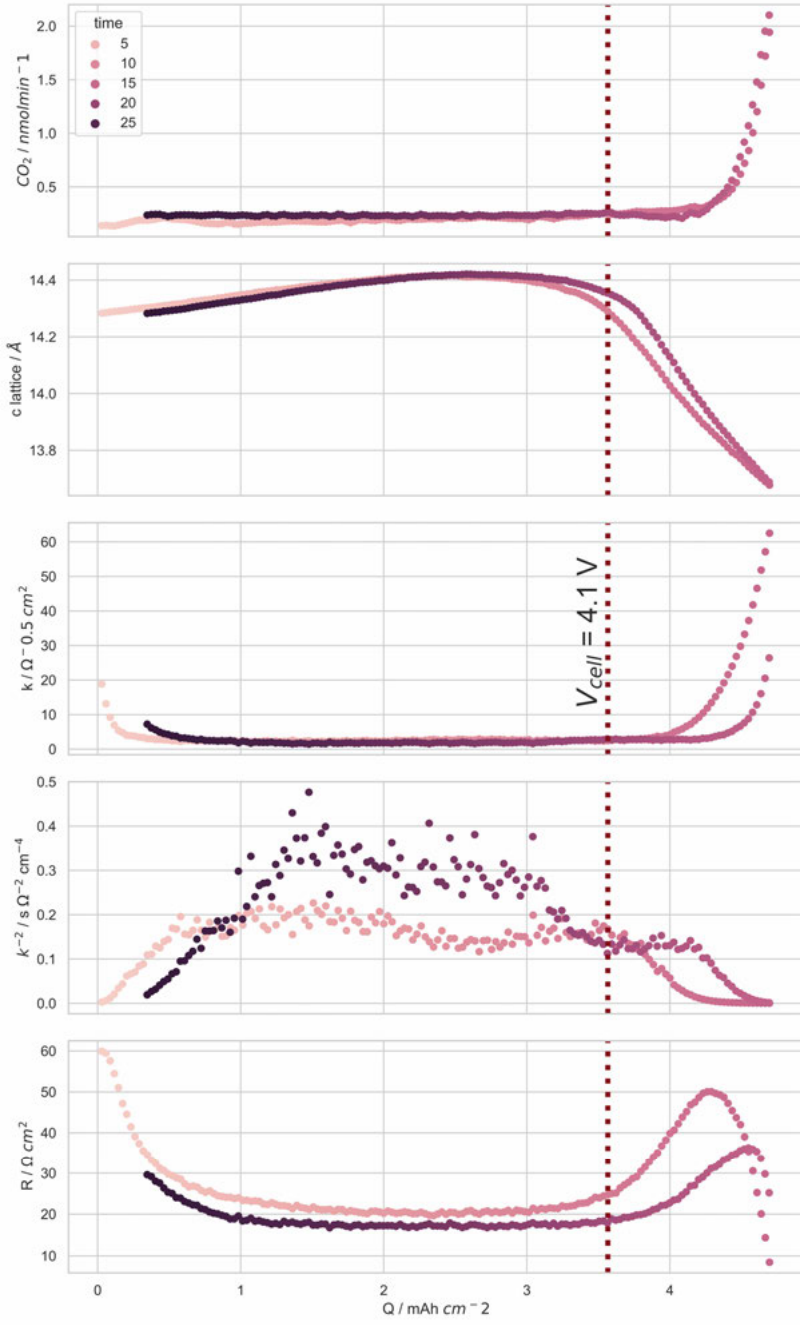


Figure 23 – Combined XRD and OEMS operando measurements. From **Paper IV**.

The following parameters were derived: $CO_2$ rate was measured using OEMS by registering channel m/z=44; *c* lattice parameter of NCA was refined from the XRD patterns collected while cycling the material; $Li^+$ diffusion resistance coefficient *k*, derived lithium diffusion approximant $k^{-2}$ and cell resistance *R* were measured using ICI cycling protocol conducted during both operando experiments. The results are displayed as a function of the normalized capacity *Q*. During delithiation, the cell operation can be divided into the standard (< 4.1 V) and high-voltage (> 4.1 V) operating conditions. In the standard region, the *c* lattice parameter first showed growth in the standard operating conditions and then collapses during the high-voltage regime during delithiation. The onset of the $Li^+$ diffusion approximant supports the dependency of the interlayer distance and $Li^+$ diffusion energy barrier shown earlier.[46] In the high voltage region, an increase in $Li^+$ diffusion resistance coefficient is followed by $CO_2$ increase. It supports the earlier reported information that the presence of molecular oxygen increases energy barriers for $Li^+$ diffusion.[130] The study (**Paper IV**) does not propose a mechanism for the $Li^+$ diffusion resistance increase as a direct correlation to molecular oxygen or *c* lattice parameter yet correlations supporting the presence of the oxygen evolution in the bulk can be observed.

Further investigation of the oxygen release was done via direct observation of the molecular oxygen formed in the bulk of electrode material using RIXS (**Paper V**). To accomplish that, RIXS measurements of the Fresh and Aged H0-100 electrodes at various states of charge were done. The O *K*-edge RIXS maps are presented in Figure 24. The fresh electrodes (BoL sample) in the lithiated and delithiated states show a striking difference in the presence of the features related to the molecular oxygen species (the magnified image is shown on the right side of Figure 24). The observation of oxygen in bulk Ni-rich materials was previously shown in Li-rich NMC[131] and NCA in potentials beyond 4.7 V.[43] The direct observation of the molecular oxygen in the working range of NCA material is shown for the first time in **Paper V**.

The observation of the molecular oxygen evolution in the aged materials was done with an *ex situ* study of the electrodes at various SoCs. The integrated spectra over the excitation energies 531.2 – 533.2 eV in Figure 24 are shown in Figure 25. An increase in the amount of the molecular oxygen with the delithiation degree is present for all samples: Fresh (BoL), Aged L (H0-50) and Aged H (H0-100). At the beginning of the delithiation Aged samples clearly show the presence of the molecular oxygen. In contrast, the Fresh sample does now show a strong feature of the molecular oxygen at the beginning of the delithiation, however this observation might be hindered due to the rising edge of the elastic peak. It is concluded that the presence of the molecular oxygen in the fresh sample is small and results from the formation cycles. A clear increase of the molecular oxygen upon delithiation is visible in the Fresh samples.

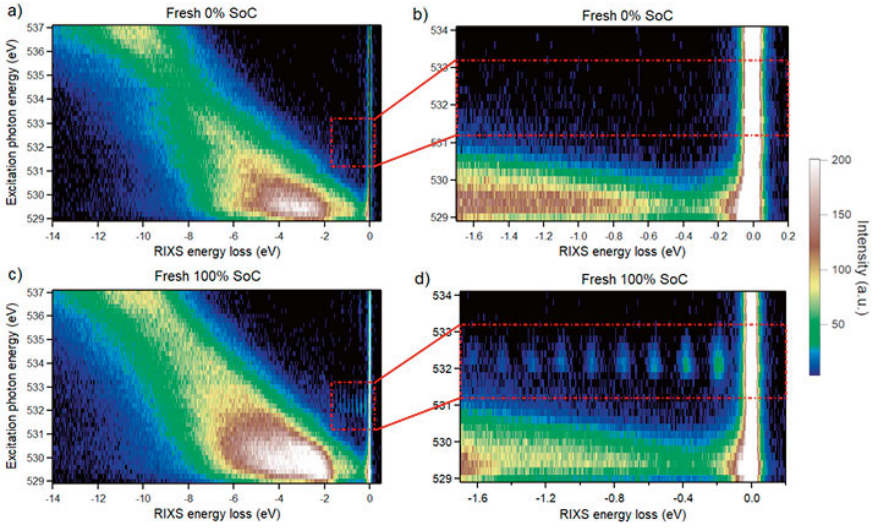


Figure 24 – Comparison of the lithiated (a) and delithiated (b) electrodes. From **Paper V**.

Comparing the samples at several stages of delithiation, the different trends are observed. At 50% SoC, the Aged L shows higher amounts of molecular oxygen compared to the Fresh sample. This might indicate that ageing promotes oxygen evolution in bulk at earlier stages of SoC. At 100% SoC, in contrast, the largest amount of bulk oxygen is detected in the Fresh sample and with both Aged samples showing lower but similar amounts. This shows that oxygen is less active in charge compensation at the high SoC in the aged materials compared to the Fresh samples.

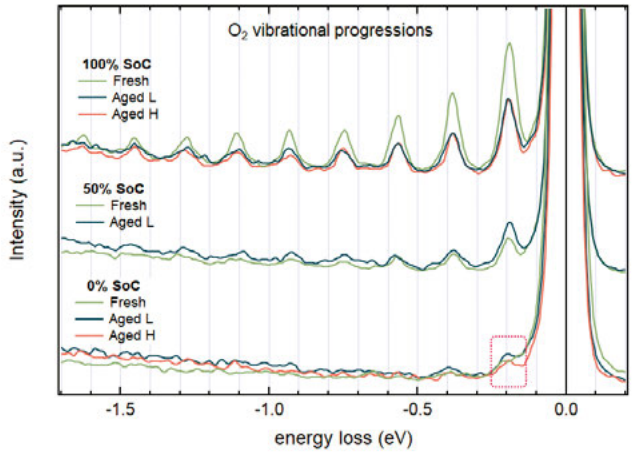


Figure 25 – O K-edge RIXS spectra displaying the region of O2 vibrations. The spectra are integrated over the excitation energies 531.2-533.2 eV. The red box accents the difference between Fresh, Aged L, and Aged H samples at 0%SoC. From **Paper V**.

Evaluating the role of oxygen is invaluable in LIBs as it helps understanding oxygen-related degradation involving both the active material and the electrolyte. Enhancing the stability and reversibility of oxygen redox reactions could pave the way for improvements towards achieving higher capacities and more stable positive electrodes.

### 4.2.5 Charge compensation in Ni-rich layered oxides and its change with ageing

The redox reaction and charge compensation are the fundamental processes in LIBs. Traditionally, it is explained as a change in the oxidation state of the transition metals.[13] However, the existence of anionic redox has now been widely discussed for an extended time, and the result of **Paper V** clearly showed that this is a process to be considered throughout the whole potential range.[43,47,132,133]An in depth evaluation of the charge compensation mechanisms for TM-$O_6$ environments was done in **Paper V** and **Paper VI**.

Initially, the *ex situ* study of the fresh and aged electrodes was done to understand the roles of transition metals and oxygen in the charge compensation during material delithiation as well as to put the perspective of the ageing at different conditions into this context (**Paper V**). The Fresh samples and the samples aged in two SoC conditions (H0-50 and H0-100) were chosen as these electrodes demonstrate similar loss in capacity. The harvested electrodes were reassembled in half-cells and delithiated to SoC = 50 and 100%. The chemical state and local environment of the transition metals was studied using XAS/EXAFS and oxygen activity was evaluated using RIXS (shown above).

The description of the changes observed in Ni, Co and O during battery operation in Fresh and Aged electrodes is schematically summarized in Figure 26. In Fresh electrodes, Ni shows the strongest change of the oxidation state accompanied by the strongest size reduction of the oxygen coordination octahedron Ni-$O_6$. In contrast, Co experiences smaller chemical state changes and lower yet present reduction of the octahedra size. At the beginning of the delithiation, the size of the Ni-$O_6$ of the octahedron is significantly larger than the Co-$O_6$. However, upon delithiation, both octahedra converge to the same size, in line with Ni-$O_6$ undergoing more significant changes. In the aged samples, the difference in octahedra sizes in the lithiated state increases compared to the Fresh sample. Such changes in octahedra sizes can promote local strains and lead to particle cracking, which is observed upon delithiation and ageing (**Paper IV**). Another important aspect is the bond hybridization which is established as another way of oxygen participation in the charge compensation.[46] Ni and Co exhibit difference in in hybridization with oxygen, where the results presented from **Paper V** indicate that stronger hybridization is found in Co-O bond than in Ni-O. This may influence the way TMs undergo ageing processes

as the local environment affects their electrochemical activity as well as local stability.

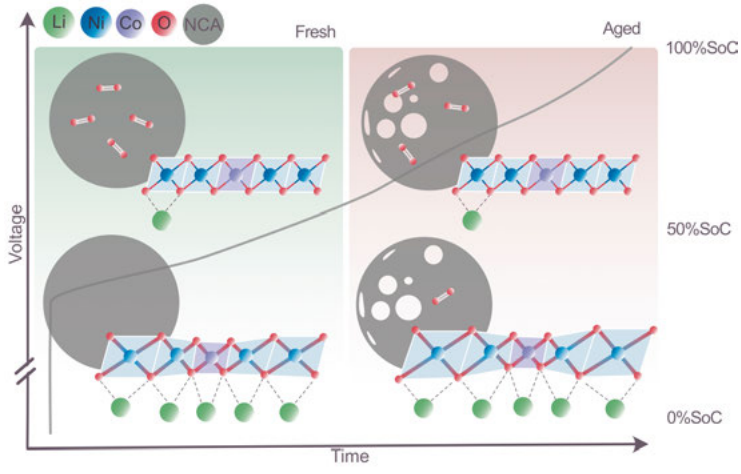


Figure 26 – The scheme of proposed charge compensation mechanism in Ni-rich electrodes. From **Paper V**.

To further understand the behaviour of the transition metals, *operando* experiments were conducted on both Fresh and Aged (H0-50 and H0-100) samples (**Paper VI**). The chemical states of Ni and Co were monitored throughout the delithiation of the NCA electrodes in Fresh, H0-50, and H0-100 materials. A linear combination analysis of the intermediate states is shown in Figure 27. The data gathered from *operando* experiments supports the findings from previous *ex situ* studies (**Paper V**), and broadens the understanding of the charge compensation process.

Figure 27 (a) displays the shift in the main absorption edge $\Delta E_0$ of Ni and Co between the initial and final states during the delithiation of the Fresh sample, obtained from a linear fit of each spectra collected *operando* by using initial and final spectra as references. A pronounced difference in the charge compensation rates and the magnitude of the shift between Ni and Co is apparent. Ni demonstrates a steady rate of oxidation, significantly surpassing that of Co until reaching ~4.0 V, at which point it markedly diminishes for Ni. By contrast, the oxidation trend for Co is semi-linear and the final oxidation state corresponds to a smaller energy shift compared to Ni. At the end of the delithiation, the shift of the Ni edge is ~30% greater than that of Co, underscoring Ni as a more pivotal charge compensator than Co. Intriguingly, in the aged cases (b) and (c), the rate of oxidation change $\Delta E_0$ for Ni and Co is more similar to each other in both H0-50 and H0-100 samples. The decrease of Co charge compensation is visible in Aged100 sample, however, the lack of

statistics at the elevated potentials does not allow to make a definite conclusion whether is it the case.

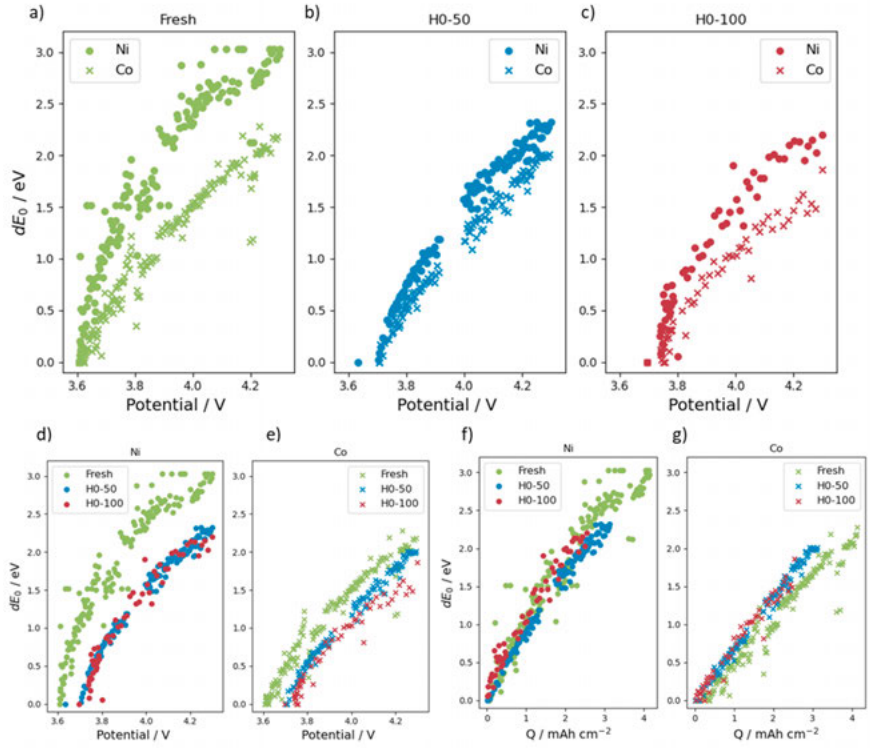


Figure 27 - Linear combination analysis of the transition from initial to final Ni and Co state in Fresh (a), H0-50(b), and H0-100(c) electrodes. Comparison of Ni and Co states in electrodes aged in various conditions as a function of half-cell potential (d and e respectively) and capacity (f and g respectively). From **Paper VI**.

To aid ageing evaluation, Figure 27 (d) and (c) compares Ni and Co in different ageing conditions as a function of the half-cell potential. In the case of Ni, the oxidation trend remains analogous for all studied conditions, despite the decrease of the total absorption edge shift by ~25%. In case of Co, the trend stays similar after the samples undergone ageing. In addition, the total $\Delta E_0$ of Co does not change significantly. However, for both Ni and Co, the shift of the measurements points towards higher potentials is observed, which is related to the electrochemical performance of the cell. This shift is due to the overpotential from formed degradation products upon ageing (**Paper I**) and local Li depletion in the material (**Paper III**). Due to the ageing, the material cannot be relithiated at the same conditions as Fresh electrode. That results in higher potential at the beginning of the delithiation. A comparison of the Ni and Co $\Delta E_0$ vs capacity is shown in Figure 27 (f) and (g) respectively. The oxidation state of the transition metals change is demonstrated to be linear

with the change of capacity. Interestingly, despite the transition metals do not exhibit significant change upon ageing, a slight difference in the activity can be observed. In particular, for Ni, only H0-50 sample has slightly decreased its activity. In case of Co, both Aged samples demonstrated higher oxidation rates upon ageing. This indicates that Co becomes more involved in the charge compensation upon ageing.

Following the charge compensation trends is crucial as it provides valuable insights for the advancement of future materials. For example, coupling various TM that could balance their respective redox activities, might be a good strategy for development of long-standing materials.

### 4.2.6 OH formation

**Paper VII** demonstrates the presence of OH-groups within the material's structure or bulk of the material. Figure 28 shows RIXS O *K*-edge heatmaps of the fresh and aged (H0-50 and H0-100) samples in lithiated and delithiated states.

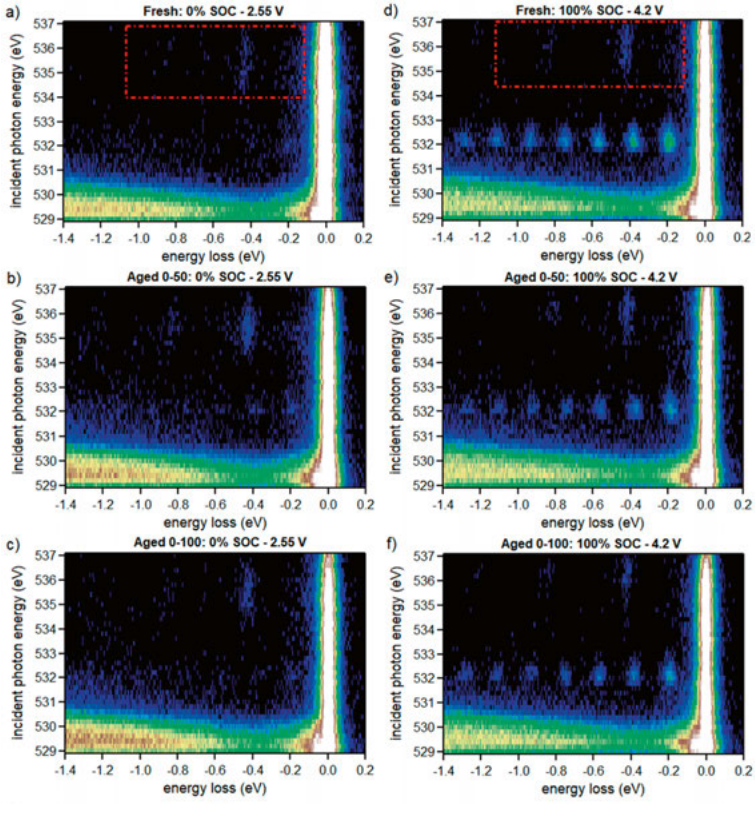


Figure 28 – O *K*-edge RIXS heatmaps of 0% (a) and 100% (d) SoC in Fresh NCA electrode; 0% (b) and 100% (e) SoC in H0-50 aged electrode and 0% (c) and 100% (f) SoC in H0-100 aged electrode. From **Paper VII**.

The vibrations of the OH-group are situated around 536 eV. The most pronounced difference in the quantity of detected OH is observed in fresh samples. Upon ageing, the quantity remains almost constant for both ageing conditions. The formation of OH is attributed to a proton-exchange mechanism.[142] Most likely, the formed OH groups are situated in the voids previously shown using TEM (**Paper VI**), and within the structure where contact with the electrolyte is limited. Interestingly, the amount of the detected OH correlates with the amounts of detected molecular oxygen (**Paper V**). It supports the suggestion of the OH formation as a reaction of the protons, produced as a result of the electrolyte decomposition, and oxygen, which evolves from the structure. These formed OH species are detrimental to the LIBs performance as they consume Li-ions, thereby diminishing the capacity of the battery.

## 4.3 Other components of LIB

The current thesis is focused on the positive electrode and, therefore, a significant part of the results discussion is focused on corresponding degradation processes. However, as shown in **Paper I**, a significant contribution of the negative electrode ageing is present. Below, the key findings of ageing of other components of LIBs are highlighted.

### 4.3.1 Negative electrode

Graphite and graphite-based composites are common negative electrode active materials.[94] The latter can have Si or $SiO_x$ as composite additives.

The ageing of the negative electrodes is usually related to the SEI, formed on the contact of the electrode with electrolyte and changing properties depending on the cycling conditions.[59,67] In the case of SiOx, the compound ageing is associated with volume expansion and reduction resulting in Li trapping, LAM due to electric disconnection, etc.[134,135]

The current study demonstrates the difference between fresh and aged negative electrodes. Cross-section SEM images were done for both cases (Figure 29). The notable SEI is formed on the SiOx particle upon its ageing. The cross-section indicates that the particle is partially disconnected from the surface. A close-up also shows that the material develops porosity within the particle. Such morphology change can affect $Li^+$ diffusion as it increases tortuosity.

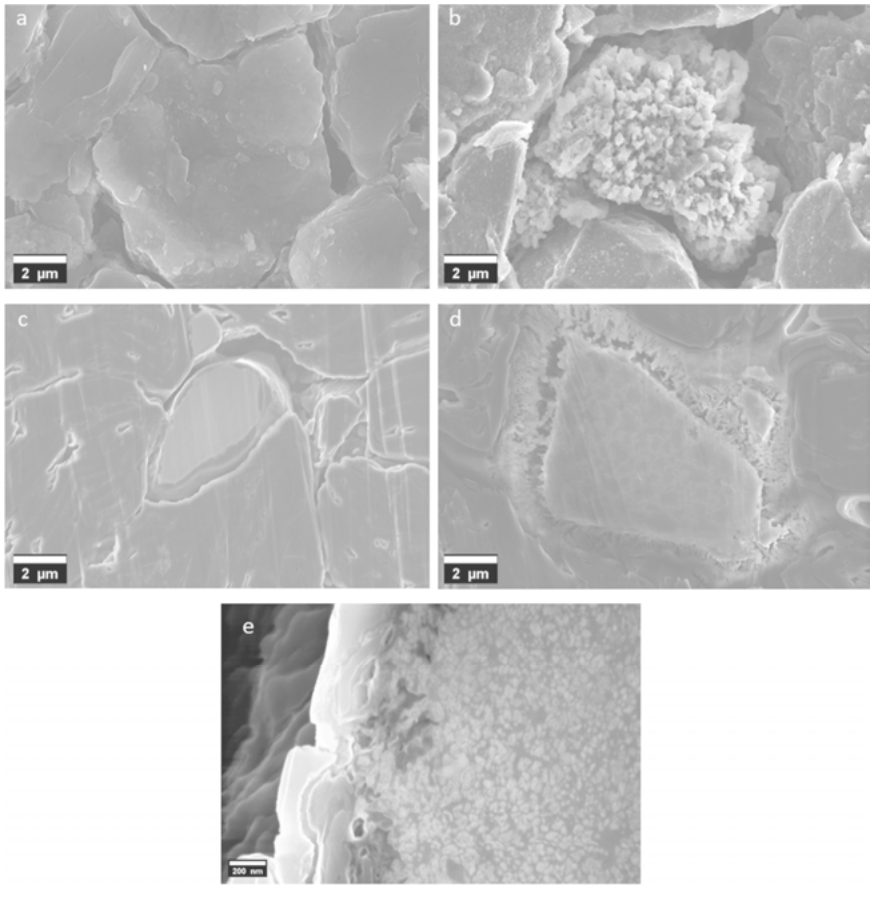


Figure 29 – SEM imaged of the negative electrodes: fresh (a, c) and aged (b, d, e). From **Paper I**.

### 4.3.2 Separator

A separator is a critical part of the Li-ion battery which is often understudied. The main function of the separator is to prevent electrical contact between the positive and negative electrodes, however, the latest trends in the separator design implement coatings that allow it to mitigate the thermal impact as well as produce scavengers upon electrolyte degradation.[136–140]

**Paper I** has investigated separators extracted from Fresh and Aged cells. Upon ageing, the amount of the pores in the separator is visibly reduced but only below a threshold of ~20 µm. This can be related to clogging of the pores with decomposition products. When local pore blockage occurs, the local resistance is increased. This result in decay in the cell performance.

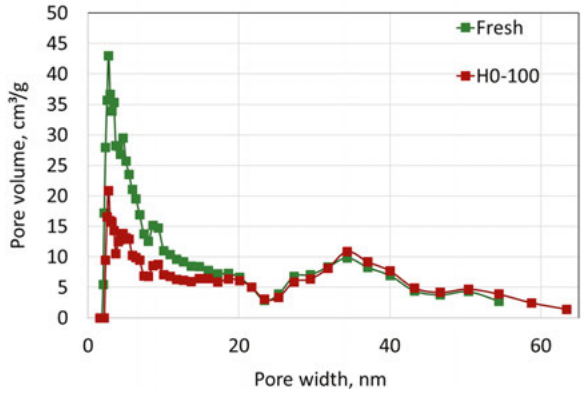


Figure 30 – Pore distribution volume of the separator extracted from fresh and aged 0-100% SoC 45°C cells. From **Paper I**.

# 5 Conclusions

The transition towards transport electrification highlights many open questions about how large format battery cells and Ni-rich NMC/NCA electrodes age given their relatively recent market introduction, which in turn strongly motivates research in this direction. A thorough understanding of these ageing processes demands a multiscale approach, combining both fundamental and applied studies.

The challenge in investigating ageing phenomena within commercial systems originates from the complex interplay of processes, coupled with the inherent limitations of the systems and existing analytical methods. The degradation issues in commercial cells start with their initial heterogeneity. When operating, the system tends to degrade faster at vulnerable regions where the stress on the system is the strongest, accelerating further degradation. The identifications of such regions are vital for designing preventive measures to extend battery life. **Papers I** and **II** showcase various heterogeneities formed upon ageing. Both cylindrical (**Paper I**) and prismatic (**Paper II**) cells exhibit a distribution in capacity loss along the length and height of the electrode roll. This underscores the need for understanding the factors provoking degradation and cell design improvements tailored to different formats.

In this thesis, the problem of heterogeneous ageing was observed across various scales. **Paper III** delves into the secondary particle level of the positive electrode material, revealing that cycling at higher SoC leads to heterogeneities in lithiation state of the material across the secondary particle, and this may possibly be linked to the higher $Li^+$ diffusion resistance in the material and performance loss shown in **Paper I**. However, cycling at slower rates of the heterogeneous materials shows improved homogeneity, suggesting that periodic slow cycling can reduce heterogeneity within the material and extend battery life.

Apart from heterogeneity within the electrode roll, degradation varies between the positive and negative electrodes, as further discussed in **Paper I**. The negative electrode capacity loss was dominant in samples reaching low SoC during cycling, correlated with the loss of electrochemically active $SiO_x$, yet the negative electrode showed fewer changes in lithium-ion diffusion resistance compared to the positive electrode. The positive electrodes, in contrast, exhibited a significant ageing dependence on both temperature and SoC. Operating at elevated temperatures and SoC conditions led to an increase in

TM dissolution and cation mixing, phenomena are expected for the Ni-rich materials. However, some of the previously reported detrimental processes were not seen to the expected extent. For example, the formation of secondary phases and particle cracking were shown to be less relevant in the examined commercial materials. This amplifies the importance of the studies conducted in close to user conditions.

The degradation processes are specific to the operating potentials. **Paper IV** shows that the increase in the $Li^+$ diffusion resistance is stronger at higher potentials and accompanied both by the decrease of the *c* lattice parameter and by $CO_2$ evolution, that originate from a side reaction of the oxygen evolved from the structure and electrolyte. These two factors are believed to be the main limitation in the extension of the Ni-rich material operation potential and are shown to be correlated in **Paper IV**. The extent of the working range of the Ni-rich TM oxides might be done by either limiting access of the evolved oxygen to electrolyte or by suppressing oxygen redox.

The understanding of the redox active species inside the material is highly important as it gives the fundamental knowledge of the battery operation. **Papers V** and **VI** were focused on understanding and resolving roles of Ni, Co and O in the charge compensation processes. Ni was found to be the main element performing charge compensation. Interestingly, the oxidation rate varies with potential. For example, the highest oxidation rate of Ni was found at lower potentials, while Co participation was found to be linear and present to lesser extent over the full voltage range. Upon ageing, the Ni becomes on average less electrochemically active with the greatest decrease in samples aged by cycling in the full SoC range. In addition, the oxidation rate of Ni slows down at lower potentials. Meanwhile in the aged samples, Co does not change significantly. A way to mitigate the Ni oxidation rate decrease might be by introducing dopants, which would create a local environment for the transition metals in a way that promotes their charge compensation activity since the environment of the atom influences on its electrochemical activity. Additionally, participation of Ni and Co in TM-O hybridization is different. Upon delithiation, hybridization decreases: Co has shown the strongest bond hybridization and hybridization change in the delithiated state, compared to Ni.

Additionally, this thesis provides insights into oxygen activities upon ageing (**Papers V** and **VI**). The participation of oxygen in charge compensation was found evident down to low potentials, documenting the first recorded formation of molecular oxygen in bulk NCA at normal operating potentials. This underlines the importance of further research into anionic redox in this type of materials. With ageing, the evolution of oxygen at higher SoC decreases. This can be a result of a change in the local environment of the atom. The material design should account for the oxygen redox as its consequences are two-fold: the increase in capacity is beneficial, while the contact of diatomic oxygen promotes electrolyte degradation (**Paper IV**). One way to mitigate such drawbacks is to develop coatings which do not evolve oxygen and protect

the contact between active material and electrolyte or to increase the electrolyte stability toward reactive oxygen. Finally, utilizing an advanced characterization technique called Resonant Inelastic X-ray Scattering (RIXS), an OH-group was identified in NCA compounds (**Paper VII**), which is presumably a product of electrolyte degradation at higher potentials. Understanding the degradation products is crucial as it reveals the processes occurring within the material.

The presented results demonstrate that the degradation is a process which is manifested at various scales. The use of the wide range of techniques allows to understand ageing and overcome technique limitations. Complementary analysis is shown to be important in connecting changes from atomic level to full cell performance decay.

In summary, this study conducted a thorough investigation into the degradation of commercial Li-ion batteries used in electric vehicles, where it is concluded that establishing correlations between processes observed at various scales is highly significant. Moreover, examining commercial materials contributes to a better understanding of relevant battery degradation. This work bridges the gap between advanced atomistic-level investigations and macro-level observations of materials in general. It emphasizes the importance of studying the role of oxygen as it is crucial both during the cell operation and its degradation. The insights gained pave the way for two major directions: improving materials and cells, and enhancing characterization methods.

Improving battery materials is a multi-faceted challenge. User requirements need to be compromised with material safety, environmental compliance, and sustainability goals. While the currently used Ni-rich layered oxide positive electrodes largely meet user needs, they demand substantial enhancements. Measures to mitigate heterogeneity at all scales are essential to extend material and battery lifespan. Additionally, doping and/or coating strategies are needed to stabilize the material at higher potentials, thereby boosting battery durability and safety. In general, a deeper understanding of redox processes at different potentials and their alterations upon ageing is crucial.

Improving characterization methods is another vital direction for future research. Analysing systems relevant to users provides deep insights into the ageing processes they are prone to. Significant challenges arise from the complexity and size of these systems, which pose limitations to many characterization methods.

In conclusion, investigating battery materials from electric cars, despite its challenges, offers abundant opportunities for multiscale and interdisciplinary research. The materials used in electric cars require improvements to ensure longer and safer operations. Challenging yet exciting times are ahead for those who works towards electrifying the world's future.

# 6 Sammanfattning

Klimatförändringar till följd av utsläpp av växthusgaser är ett av vår tids största problem. Ett viktigt område där utsläppen kan minskas är transportsektorn, som just nu genomgår en snabb förändring där fossila drivmedel byts ut mot elektriskt drivmedel. Litiumjonbatteriet (LIB) är i dagsläget en förutsättning för den utvecklingen då det har möjlighet att lagra en tillräckligt stor mängd energi per vikt och volym för att användas i elbilar. Tyvärr tenderar LIB att försämras med tiden, vilket slutligen leder till att batteriet behöver bytas ut. Detta är inte enbart kostsamt för konsumenten, utan ökar också den negativa påverkan som exempelvis tillverkning av LIB har på miljön. Den här avhandlingen fokuserar på att ge en ökad förståelse för försämringen av positiva elektroders aktiva material, främst $LiNiCoMnO_2$ och $LiNiCoAlO_2$ från kommersiellt tillgängliga batterier i elbilar.

Många nedbrytningsmekanismer är kända sedan tidigare: aktivt material kan bli inaktivt på grund av förlorad elektrisk kontakt med resten av elektroden, vissa atomer kan lämna den aktiva strukturen eller omorganiseras på ett sätt som gör att materialet inte längre fungerar optimalt, och ibland kan materialet brytas ner via oönskade kemiska reaktioner och bl.a. orsaka att materialet släpper ifrån sig gas. Alla dessa processer är negativa för batteriets funktion, inte bara för batteriets livstid utan också för dess säkerhet. Säkerheten hos batterier är extra viktig eftersom många av de används i närheten av människor. För att förbättra dessa batterier är det avgörande att förstå hur batterikomponenterna bryts ner.

De huvudsakliga komponenterna i ett litiumjonbatteri inkluderar en positiv och en negativ elektrod, en separator och en elektrolyt. Energin omvandlas via redoxreaktioner vid elektrodernas ytor och lagras i de aktiva materialen i elektroderna. Det finns många olika typer av aktiva elektrodmaterial, var och en med sina fördelar och nackdelar. $LiNiCoMnO_2$ och $LiNiCoAlO_2$ är två exempel på aktivt material som används i den positiva elektroden i de litiumjonbatterier som finns tillgängliga på marknaden idag, och tillika de material som står i fokus för den här avhandlingen.

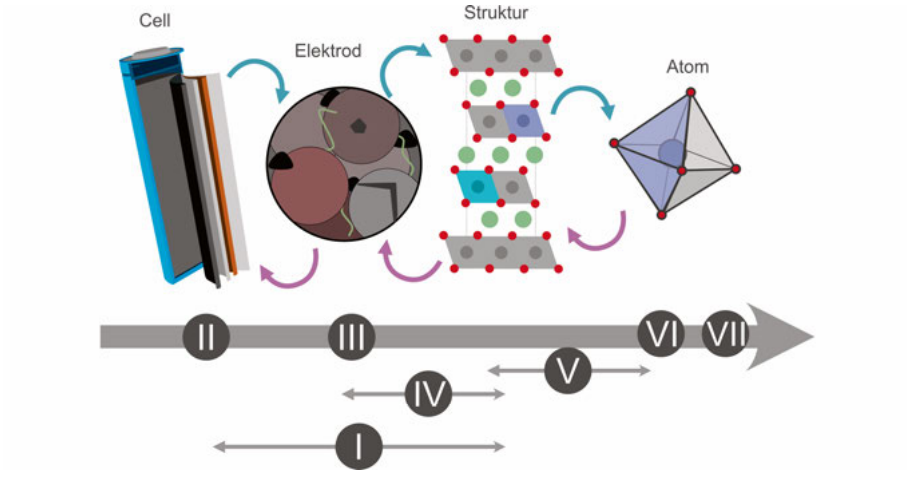


Figur 1. Sammanfattning av de artiklar som ligger till grund för avhandlingen.

Sju artiklar ligger till grund för avhandlingen och de sammanfattas schematiskt i figur 1 samt i texten nedan. Avhandlingen tar sitt avstamp i en studie av hur de hela batteriernas prestanda försämras på grund av olika förhållanden under användning, där parametrar som temperatur och spänningsfönster varierades. För att vidare förstå var och varför försämringen inträffar, demonterades batterierna och dess komponenter analyserades oberoende av varandra. Resultaten visar att en försämrad prestanda huvudsakligen kommer från oönskade sidoreaktioner vid den negativa elektroden. Dock spelar försämringen av den positiva elektroden en betydande roll, särskilt för de batterier som använts vid högre temperaturer.

Den andra studien syftar till att identifiera om några delar av elektroderna försämras mer än andra. I en tidigare studie identifierade allvarlig litiumplätering inuti dessa typer av batterier. På grund av den betydande mängd material som bygger upp batteriet kan man inte alltid använda standardmetoder för att analysera intakta större batterier. Detta gäller speciellt när man är intresserad av att se heterogeniteter i batteriets material. I studien användes röntgendiffraktion (diffraktionsradiografi), för att erhålla en millimeterupplöst 2D-visualisering av de aktiva materialen. Undersökningen genomfördes i det lodräta planet genom batteriet, i ett batteri där kapaciteten hade sjunkit under 80% av den initiala kapaciteten. Resultaten visar bl.a att den positiva elektroden kan fungera under förhållanden där litiumplätering skett på motstående område på anoden. Den andra artikeln påvisade heterogeniteter i åldringen av batterier på millimeterskala, dock finns några av heterogeniteterna på en mycket mindre skala. Exempelvis behandlar studien i den tredje artikeln en enskild partikel av det positiva elektrodaktiva materialet. Genom att använda samma metod (röntgendiffraktion), men där mätpunkten är i nano-storlek, visas att lititeringsgraden också varierar i olika delar av partikeln. Resultaten visar även

att efter omfattande åldrande, kan långsam cykling till viss del bidra till att homogenisera sådana skillnader.

Vidare fokuserar avhandlingen på specifika åldringsmekanismer som finns hos de positiva elektrodmaterialen. Den fjärde artikeln presenterar en analys av gasutveckling från den positiva elektroden och undersöker dess korrelation till strukturella förändringar som förekommer i den positiva elektrodens bulk. Där påvisades att samtidigt som materialets struktur förändrades ökar motståndet för litiumdiffusion i materialet och en gasutveckling sker. Vidare observerades koldioxid, som är en produkt när syre reagerar med elektrolyten. Syrets roll i det aktiva materialet är i fokus för den femte artikeln, och den avslöjar att bland annat att syre är delaktigt i laddningskompensationen. Även om syret är bundet till övergångsmetallerna, visar resultaten att bindningens karaktär skiljer sig för Ni och Co, och att detta leder till en viss skillnad i mekanismen för laddningskompensation för dessa ämnen. Vidare visar resultaten i studie fem att molekylärt syre utvecklas reversibelt i det aktiva materialets struktur i ett större spänningsområde än tidigare känt. Å ena sidan, utökar formering av molekylärt syre den energi som materialet kan leverera, men å andra sidan kan det minska stabiliteten hos det aktiva materialets struktur. Dessutom reagerar utvecklat syre med elektrolyten när de är i kontakt. En annan intressant observation i avhandlingen var bildning av porer inuti det positiva elektrodmaterialet. Porbildning bör ändra de mekaniska egenskaperna hos materialet och även påverka litiumdiffusionen, där båda faktorerna kommer att påverka batteriprestandan negativt. Den sjätte artikeln behandlar laddningskompensationen i övergångsmetallerna Ni och Co. Ni är relativt Co initialt dominerande som laddningskompenserare. I det åldrade materialet minskar laddningskompensationen för Ni medan laddningskompensationen för Co till större del bevarats. Den sjunde och sista artikeln ägnades åt nedbrytningsprodukter som hittades inuti cellen. Genom att använda en avancerad karakteriseringsteknik som kallas resonant inelastisk röntgenspridning (resonant inelastic X-ray scattering, RIXS), identifierades en OH-grupp i NCA-materialet, vilket troligen är en produkt av elektrolytnedbrytning vid högre potentialer.

Sammanfattningsvis genomfördes ett djupgående arbete med att identifiera mekanismerna bakom försämringen av kommersiella Li-jonbatterier för elbilar. Avhandlingen använder en kombination av avancerade tekniker som ger information på atomistisk nivå och tekniker som ger information på en makroskopisk nivå. I avhandlingen undersöks material från kommersiella batterier, vilket bryggar över från mindre modellbatterier, som ofta används inom akademisk forskning, till att förstå hur större batterier kan försämras i kommersiella applikationer som exempelvis elbilar.

# 7 Acknowledgements

*"There is an art, or, rather, a knack to flying.*
*The knack lies in learning how to throw yourself at the ground and miss."*
*The Hitchhiker's Guide to the Galaxy, Douglas Adams*

This work, both shown in this thesis and hidden for now behind the lines of "outlook", is a result of joined efforts. It is all done through rigorous beamtimes, impromptu discussions, short and long Zoom meetings (Your mic is off! What? Aah, mine too…), countless emails, and also fun trips, parties, highs and lows, but mostly, through all the small things that just go on from day to day. It's been a life-changing four years and now, at the very last minute, I am anxiously going through my notes, fully aware that I am forgetting half, so I will try to keep it short.

First and foremost, my huge gratitude goes to all of my supervisors. Maria, you have been an exceptional person to look up to. I deeply appreciate all the opportunities you gave me, I am very lucky to be a student who was rewarded with so much freedom and resources, chances to enjoy conferences, summer schools, and beamtimes. You created a safe space where it was natural to grow and glow and I just wish our paths had crossed earlier. Matt "the Architect" Lacey, thank you for all the great discussions, and cell teardowns and for showing me research in the industry. Thank you also for your kindness and patience. It felt inspiring to see your legacy in the lab even though I joined a bit later. It is also moving to see your efforts in making the battery field a better place. You are truly an inspiring person. I would also like to thank Cesar for fruitful discussions and creative methods, you are a kind person and a great and patient teacher. I wish I had more opportunities to learn crystallography from you.

Connecting academia and industry is a silver lining throughout my thesis and that is possible because of the great ALINE project I was a part of. During the project, we had many fruitful collaborations, academia/industry discussions and fun activities and I will take this experience with me. I would like to thank especially those, who endured with me through the frustrating world of analysing commercial cells. Alex S and Kristian, I am grateful we stood together in a hard/fun time. I am also grateful to Niladri, Istaq, Torbjörn, Rakel and all ALINE partners, who worked on the project. We did a work that makes me feel proud.

I cannot leave this acknowledgement without at least a paragraph to the "oxygen" team. I am grateful to Laurent, Moritz, and Pontus for introducing me to the vibrant world of RIXS. Soham, thank you for your patience with my hundreds of spectra and thousands of questions. I am also grateful to Cheuk-Wai for the beautiful world of TEM and unexpected findings and nice discussions. Thanks also to Håkan for some challenging questions. I learnt a lot from all of you and this collaboration (and all the countless spinoffs it is still generating) means a lot to me.

Thanks to "X-rays for batteries" team for meetings, discussions, fikas and beamtime planning. With all your enthusiasm, I never got tired of learning of all the many ways we can use X-rays. Thanks to Will for generously sharing beamtimes, I enjoyed working on the outcomes and there is so much more yet to come. Also, thanks to Heyin, Qianhui and Raheleh, who always found time to join and support my beamtime activities. Thanks to Alexander Schökel for the fastest feedback! Thanks to all beamline scientists, I deeply appreciate your support, help, and engagement.

Thanks to all co-authors of the papers: I counted at least 37 people in the main paper list. A huge thank you to all of you! My favourite part was always discussions and I am grateful to everyone who was engaged, asked difficult questions, shared their thoughts and found time for last-minute feedback.

I would also like to thank all my past and present colleagues from the Ångström Advanced Battery Research Centre who made efforts to make our lab environment better. Thanks to Kristina and Daniel for keeping the ÅABC running – it is a good place to do battery science. A special line to the present and past lab managers: Alina(!), Fredrik, Long, and Henrik, our lab is/was standing on your shoulders. Thanks to Leif from the workshop who always managed to help on very short notice. A big part of my thesis was me locked for hours in the cleanroom: thanks to Amit, Olivier and Fredrik for all the fun I had with microscopy/FIB/ion-polishing. Thanks to the Chemistry PhD student Council – I am proud that we started the challenging road even though there is a long way to go. I am also happy to become the first ombudsperson of the Chemistry Department together with Matina – it was a learning curve, which was completely worth it and good luck to Meghdad, the next one in line. Thanks to the Equal Opportunity Group – I appreciated the discussions and the projects that were organized – I learned a lot. And last, but not least, I cannot end the official part without mentioning just a few more names: Funeka, thank you for being a lovely office mate and wish you all the best with your new important responsibility. Alex U, thank you for being a nice landscape neighbour, a great baker and a kind person. Yu-Kai, you were late for just one day… Florian Twist, Wessel – I am still surprised we survived the storm and thanks to Killian for never doubting us. Thanks to Edvin for juggling teaching with me. Thanks to Nataliia for being an inspiring person. Thank you to all those who made this place welcoming and fun and a shutout to the Glamscape mates: no matter how many flies can be on our way, we can do it!

When I came to Sweden to start my PhD, the last thing I thought about was how socially active these years would be. I am grateful to everyone, who bonded over PhD time with me through board games, and parties, and weird quizzes, and movie nights, and hikes, and improv. I am especially thankful to all the great people who supported me and shared with me these years full of craziness: Pier, Miora, Philipp, Matias, Rafael, Zahra, Reza, Fernand and Diego, thank you for all the fun things we did together. I cannot imagine Uppsala without you. You added colours to this place. Thanks to Violeta, Simon, Patrik and the board game crew – why do I always win? I am sure the games are rigged. Or my memory. Thanks to Anna and Eike for the nice time and more board games. The once I never win. Thanks to Benedict, Maria, Joona, and the ice-cream people for all the random zoom games, trips and unexpected news.

I cannot leave this section without a shutout to my co-host Daria (good luck with your thesis!) and all followers of our podcast. It was an eventful journey and I am happy to have so many supporters who went all this way with me.

Oxana, thank you for our connection through the years and for reminding me how far we've come. I admire you as a friend, as a musician, as a teacher, as an artist and as someone who has known me for almost two decades and is always there to support me. Miss you tons!

A line here goes to the star of my cover – Tiramisu McThompson, but you won't read it anyway so why bother?

Thanks to my great grandma who kept saying "Don't let her read so much, she will go crazy" and to my parents, who kept bringing me new books. I guess, I agree that there is no point in staying sane. But seriously, thanks to my parents who are a great example to me and who always cherished and supported my drive to learn and were never surprised but surprisingly supportive of my ideas, projects and ambitions. You are my best team! Love you and can't wait to see you again one day.

And last, but not least, to the person who held the walls of my mind castle from turning into Mojo Dojo Casa House, Ignacio. Once you said "Nothing is so important" and this is still keeping me standing when the world is crushing over and over. I am happy to have you by my side during all these times and I cannot describe, how great it feels to have you as a person I could rely on. Thank you for your wisdom, and your patience, and your positivity. I am learning a lot from you every day. Your ability to create an amazing artistic free-thinking space and your magnetism to attract the best kind of people are what actually kept me happy during this time. I cannot count how many fun gigs you have organized and I am happy to be a part of it. Thank you for all the great adventures! What's next?

# 8 References


(1) Abrahms, B.; Carter, N. H.; Clark-Wolf, T. J.; Gaynor, K. M.; Johansson, E.; McInturff, A.; Nisi, A. C.; Rafiq, K.; West, L. Climate Change as a Global Amplifier of Human–Wildlife Conflict. *Nat. Clim. Change* **2023**, *13* (3), 224–234. https://doi.org/10.1038/s41558-023-01608-5.

(2) Fetting, C. *The European Green Deal*; ESDN Office, Vienna, 2020.

(3) Abram, N. J.; McGregor, H. V.; Tierney, J. E.; Evans, M. N.; McKay, N. P.; Kaufman, D. S. Early Onset of Industrial-Era Warming across the Oceans and Continents. *Nature* **2016**, *536* (7617), 411–418. https://doi.org/10.1038/nature19082.

(4) Fleming, J. R. Joseph Fourier, the 'Greenhouse Effect', and the Quest for a Universal Theory of Terrestrial Temperatures. *Endeavour* **1999**, *23* (2), 72–75. https://doi.org/10.1016/S0160-9327(99)01210-7.

(5) Uppenbrink, J. Arrhenius and Global Warming. *Science* **1996**, *272* (5265), 1122–1122. https://doi.org/10.1126/science.272.5265.1122.

(6) *What is the United Nations Framework Convention on Climate Change? | UNFCCC*. https://unfccc.int/process-and-meetings/what-is-the-united-nations-framework-convention-on-climate-change (accessed 2023-06-27).

(7) *Katowice climate package | UNFCCC*. https://unfccc.int/process-and-meetings/the-paris-agreement/the-katowice-climate-package/katowice-climate-package (accessed 2023-06-27).

(8) *THE 17 GOALS | Sustainable Development*. https://sdgs.un.org/goals (accessed 2023-06-27).

(9) *Fit for 55*. https://www.consilium.europa.eu/en/policies/green-deal/fit-for-55-the-eu-plan-for-a-green-transition/ (accessed 2023-06-27).

(10) Kapustin, N. O.; Grushevenko, D. A. Long-Term Electric Vehicles Outlook and Their Potential Impact on Electric Grid. *Energy Policy* **2020**, *137*, 111103. https://doi.org/10.1016/j.enpol.2019.111103.

(11) Ajanovic, A. The Future of Electric Vehicles: Prospects and Impediments. *WIREs Energy Environ.* **2015**, *4* (6), 521–536. https://doi.org/10.1002/wene.160.

(12) Høyer, K. G. The History of Alternative Fuels in Transportation: The Case of Electric and Hybrid Cars. *Util. Policy* **2008**, *16* (2), 63–71. https://doi.org/10.1016/j.jup.2007.11.001.

(13) Li, M.; Lu, J.; Chen, Z.; Amine, K. 30 Years of Lithium-Ion Batteries. *Adv. Mater.* **2018**, *30* (33), 1800561. https://doi.org/10.1002/adma.201800561.
(14) Kurzweil, P. Gaston Planté and His Invention of the Lead–Acid Battery—The Genesis of the First Practical Rechargeable Battery. *J. Power Sources* **2010**, *195* (14), 4424–4434. https://doi.org/10.1016/j.jpowsour.2009.12.126.
(15) Anderson, C. D.; Anderson, J. *Electric and Hybrid Cars: A History, 2d Ed.*; McFarland, 2010.
(16) *Global EV Outlook 2023 – Analysis*. IEA. https://www.iea.org/reports/global-ev-outlook-2023 (accessed 2023-06-27).
(17) Deng, J.; Bae, C.; Denlinger, A.; Miller, T. Electric Vehicles Batteries: Requirements and Challenges. *Joule* **2020**, *4* (3), 511–515. https://doi.org/10.1016/j.joule.2020.01.013.
(18) Frith, J. T.; Lacey, M. J.; Ulissi, U. A Non-Academic Perspective on the Future of Lithium-Based Batteries. *Nat. Commun.* **2023**, *14* (1), 420. https://doi.org/10.1038/s41467-023-35933-2.
(19) El Kharbachi, A.; Zavorotynska, O.; Latroche, M.; Cuevas, F.; Yartys, V.; Fichtner, M. Exploits, Advances and Challenges Benefiting beyond Li-Ion Battery Technologies. *J. Alloys Compd.* **2020**, *817*, 153261. https://doi.org/10.1016/j.jallcom.2019.153261.
(20) Rudola, A.; Sayers, R.; Wright, C. J.; Barker, J. Opportunities for Moderate-Range Electric Vehicles Using Sustainable Sodium-Ion Batteries. *Nat. Energy* **2023**, *8* (3), 215–218. https://doi.org/10.1038/s41560-023-01215-w.
(21) *The Nobel Prize in Chemistry 2019*. NobelPrize.org. https://www.nobelprize.org/prizes/chemistry/2019/popular-information/ (accessed 2023-06-27).
(22) *Lithium-ion Battery Market Size, Share [2023 Trends Report]*. https://www.grandviewresearch.com/industry-analysis/lithium-ion-battery-market (accessed 2023-06-27).
(23) Liu, C.; Neale, Z. G.; Cao, G. Understanding Electrochemical Potentials of Cathode Materials in Rechargeable Batteries. *Mater. Today* **2016**, *19* (2), 109–123. https://doi.org/10.1016/j.mattod.2015.10.009.
(24) Yuan, L.-X.; Wang, Z.-H.; Zhang, W.-X.; Hu, X.-L.; Chen, J.-T.; Huang, Y.-H.; Goodenough, J. B. Development and Challenges of LiFePO4 Cathode Material for Lithium-Ion Batteries. *Energy Environ. Sci.* **2011**, *4* (2), 269–284. https://doi.org/10.1039/C0EE00029A.
(25) Osiak, M.; Geaney, H.; Armstrong, E.; O'Dwyer, C. Structuring Materials for Lithium-Ion Batteries: Advancements in Nanomaterial Structure, Composition, and Defined Assembly on Cell Performance. *J. Mater. Chem. A* **2014**, *2* (25), 9433–9460. https://doi.org/10.1039/C4TA00534A.
(26) Liu, D.-H.; Bai, Z.; Li, M.; Yu, A.; Luo, D.; Liu, W.; Yang, L.; Lu, J.; Amine, K.; Chen, Z. Developing High Safety Li-Metal Anodes for

Future High-Energy Li-Metal Batteries: Strategies and Perspectives. *Chem. Soc. Rev.* **2020**, *49* (15), 5407–5445. https://doi.org/10.1039/C9CS00636B.

(27) Zhang, H.; Yang, Y.; Ren, D.; Wang, L.; He, X. Graphite as Anode Materials: Fundamental Mechanism, Recent Progress and Advances. *Energy Storage Mater.* **2021**, *36*, 147–170. https://doi.org/10.1016/j.ensm.2020.12.027.

(28) Zhao, L.; Ding, B.; Qin, X.-Y.; Wang, Z.; Lv, W.; He, Y.-B.; Yang, Q.-H.; Kang, F. Revisiting the Roles of Natural Graphite in Ongoing Lithium-Ion Batteries. *Adv. Mater.* **2022**, *34* (18), 2106704. https://doi.org/10.1002/adma.202106704.

(29) Asenbauer, J.; Eisenmann, T.; Kuenzel, M.; Kazzazi, A.; Chen, Z.; Bresser, D. The Success Story of Graphite as a Lithium-Ion Anode Material – Fundamentals, Remaining Challenges, and Recent Developments Including Silicon (Oxide) Composites. *Sustain. Energy Fuels* **2020**, *4* (11), 5387–5416. https://doi.org/10.1039/D0SE00175A.

(30) Liu, Z.; Yu, Q.; Zhao, Y.; He, R.; Xu, M.; Feng, S.; Li, S.; Zhou, L.; Mai, L. Silicon Oxides: A Promising Family of Anode Materials for Lithium-Ion Batteries. *Chem. Soc. Rev.* **2019**, *48* (1), 285–309. https://doi.org/10.1039/c8cs00441b.

(31) An, J.; Shi, L.; Chen, G.; Li, M.; Liu, H.; Yuan, S.; Chen, S.; Zhang, D. Insights into the Stable Layered Structure of a Li-Rich Cathode Material for Lithium-Ion Batteries. *J. Mater. Chem. A* **2017**, *5* (37), 19738–19744. https://doi.org/10.1039/C7TA05971J.

(32) Li, Q.; Ning, D.; Wong, D.; An, K.; Tang, Y.; Zhou, D.; Schuck, G.; Chen, Z.; Zhang, N.; Liu, X. Improving the Oxygen Redox Reversibility of Li-Rich Battery Cathode Materials via Coulombic Repulsive Interactions Strategy. *Nat. Commun.* **2022**, *13* (1), 1123. https://doi.org/10.1038/s41467-022-28793-9.

(33) House, R. A.; Rees, G. J.; Pérez-Osorio, M. A.; Marie, J.-J.; Boivin, E.; Robertson, A. W.; Nag, A.; Garcia-Fernandez, M.; Zhou, K.-J.; Bruce, P. G. First-Cycle Voltage Hysteresis in Li-Rich 3d Cathodes Associated with Molecular O2 Trapped in the Bulk. *Nat. Energy* **2020**, *5* (10), 777–785. https://doi.org/10.1038/s41560-020-00697-2.

(34) Liu, D.; Zhu, W.; Trottier, J.; Gagnon, C.; Barray, F.; Guerfi, A.; Mauger, A.; Groult, H.; M. Julien, C.; B. Goodenough, J.; Zaghib, K. Spinel Materials for High-Voltage Cathodes in Li-Ion Batteries. *RSC Adv.* **2014**, *4* (1), 154–167. https://doi.org/10.1039/C3RA45706K.

(35) Tran, M.-K.; DaCosta, A.; Mevawalla, A.; Panchal, S.; Fowler, M. Comparative Study of Equivalent Circuit Models Performance in Four Common Lithium-Ion Batteries: LFP, NMC, LMO, NCA. *Batteries* **2021**, *7* (3), 51. https://doi.org/10.3390/batteries7030051.

(36) Xu, C.; Dai, Q.; Gaines, L.; Hu, M.; Tukker, A.; Steubing, B. Future Material Demand for Automotive Lithium-Based Batteries. *Commun.*

*Mater. 2020 11* **2020**, *1* (1), 1–10. https://doi.org/10.1038/s43246-020-00095-x.

(37) Mizushima, K.; Jones, P. C.; Wiseman, P. J.; Goodenough, J. B. LixCoO2 (0<x<-1): A New Cathode Material for Batteries of High Energy Density. *Mater. Res. Bull.* **1980**, *15* (6), 783–789. https://doi.org/10.1016/0025-5408(80)90012-4.

(38) Huang, Y. The Discovery of Cathode Materials for Lithium-Ion Batteries from the View of Interdisciplinarity. *Interdiscip. Mater.* **2022**, *1* (3), 323–329. https://doi.org/10.1002/idm2.12048.

(39) Zhang, Z.; Meng, Y.; Xiao, D. Tri-Sites Co-Doping: An Efficient Strategy towards the Realization of 4.6V-LiCoO2 with Cyclic Stability. *Energy Storage Mater.* **2023**, *56*, 443–456. https://doi.org/10.1016/j.ensm.2023.01.019.

(40) Wang, T.; Luo, H.; Fan, J.; Thapaliya, B. P.; Bai, Y.; Belharouak, I.; Dai, S. Flux Upcycling of Spent NMC 111 to Nickel-Rich NMC Cathodes in Reciprocal Ternary Molten Salts. *iScience* **2022**, *25* (2), 103801. https://doi.org/10.1016/j.isci.2022.103801.

(41) Heenan, T. M. M.; Wade, A.; Tan, C.; Parker, J. E.; Matras, D.; Leach, A. S.; Robinson, J. B.; Llewellyn, A.; Dimitrijevic, A.; Jervis, R.; Quinn, P. D.; Brett, D. J. L.; Shearing, P. R. Identifying the Origins of Microstructural Defects Such as Cracking within Ni-Rich NMC811 Cathode Particles for Lithium-Ion Batteries. *Adv. Energy Mater.* **2020**, *10* (47), 2002655. https://doi.org/10.1002/aenm.202002655.

(42) Li, T.; Yuan, X.-Z.; Zhang, L.; Song, D.; Shi, K.; Bock, C. *Degradation Mechanisms and Mitigation Strategies of Nickel-Rich NMC-Based Lithium-Ion Batteries*; Springer Singapore, 2019; Vol. 2018. https://doi.org/10.1007/s41918-019-00053-3.

(43) Lebens-Higgins, Z. W.; Faenza, N. V.; Radin, M. D.; Liu, H.; Sallis, S.; Rana, J.; Vinckeviciute, J.; Reeves, P. J.; Zuba, M. J.; Badway, F.; Pereira, N.; Chapman, K. W.; Lee, T. L.; Wu, T.; Grey, C. P.; Melot, B. C.; Van Der Ven, A.; Amatucci, G. G.; Yang, W.; Piper, L. F. J. Revisiting the Charge Compensation Mechanisms in LiNi0.8Co0.2-: YAlyO2 Systems. *Mater. Horiz.* **2019**, *6* (10), 2112–2123. https://doi.org/10.1039/c9mh00765b.

(44) Laubach, S.; Laubach, S.; Schmidt, P. C.; Ensling, D.; Schmid, S.; Jaegermann, W.; Thißen, A.; Nikolowski, K.; Ehrenberg, H. Changes in the Crystal and Electronic Structure of LiCoO2 and LiNiO2 upon Li Intercalation and De-Intercalation. *Phys. Chem. Chem. Phys.* **2009**, *11* (17), 3278–3289. https://doi.org/10.1039/B901200A.

(45) Liu, X.; Liu, T.; Wang, R.; Cai, Z.; Wang, W.; Yuan, Y.; Shahbazian-Yassar, R.; Li, X.; Wang, S.; Hu, E.; Yang, X.-Q.; Xiao, Y.; Amine, K.; Lu, J.; Sun, Y. Prelithiated Li-Enriched Gradient Interphase toward Practical High-Energy NMC–Silicon Full Cell. *ACS Energy Lett.* **2021**, *6* (2), 320–328. https://doi.org/10.1021/acsenergylett.0c02487.

(46) Kleiner, K.; Murray, C. A.; Grosu, C.; Ying, B.; Winter, M.; Nagel, P.; Schuppler, S.; Merz, M. On the Origin of Reversible and Irreversible Reactions in LiNi x Co (1−x)/2 Mn (1−x)/2 O 2. *J. Electrochem. Soc.* **2021**, *168* (12), 120533. https://doi.org/10.1149/1945-7111/ac3c21.
(47) Li, M.; Liu, T.; Bi, X.; Chen, Z.; Amine, K.; Zhong, C.; Lu, J. Cationic and Anionic Redox in Lithium-Ion Based Batteries. *Chem. Soc. Rev.* **2020**, *49* (6), 1688–1705. https://doi.org/10.1039/C8CS00426A.
(48) Assat, G.; Tarascon, J.-M. Fundamental Understanding and Practical Challenges of Anionic Redox Activity in Li-Ion Batteries. *Nat. Energy* **2018**, *3* (5), 373–386. https://doi.org/10.1038/s41560-018-0097-0.
(49) Liu, J.; Du, Z.; Wang, X.; Tan, S.; Wu, X.; Geng, L.; Song, B.; Chien, P.-H.; Michelle Everett, S.; Hu, E. Anionic Redox Induced Anomalous Structural Transition in Ni-Rich Cathodes. *Energy Environ. Sci.* **2021**, *14* (12), 6441–6454. https://doi.org/10.1039/D1EE02987H.
(50) Qiu, B.; Zhang, M.; Lee, S.-Y.; Liu, H.; Wynn, T. A.; Wu, L.; Zhu, Y.; Wen, W.; Brown, C. M.; Zhou, D.; Liu, Z.; Meng, Y. S. Metastability and Reversibility of Anionic Redox-Based Cathode for High-Energy Rechargeable Batteries. *Cell Rep. Phys. Sci.* **2020**, *1* (3), 100028. https://doi.org/10.1016/j.xcrp.2020.100028.
(51) Palomares, V.; Nieto, N.; Rojo, T. Negative Electrode Materials for High-Energy Density Li- and Na-Ion Batteries. *Curr. Opin. Electrochem.* **2022**, *31*, 100840. https://doi.org/10.1016/j.coelec.2021.100840.
(52) Xing, J.; Bliznakov, S.; Bonville, L.; Oljaca, M.; Maric, R. A Review of Nonaqueous Electrolytes, Binders, and Separators for Lithium-Ion Batteries. *Electrochem. Energy Rev.* **2022**, *5* (4), 14. https://doi.org/10.1007/s41918-022-00131-z.
(53) Xu, K. Electrolytes and Interphases in Li-Ion Batteries and Beyond. *Chem. Rev.* **2014**, *114* (23), 11503–11618. https://doi.org/10.1021/cr500003w.
(54) Scrosati, B. Recent Advances in Lithium Ion Battery Materials. *Electrochimica Acta* **2000**, *45* (15), 2461–2466. https://doi.org/10.1016/S0013-4686(00)00333-9.
(55) Wang, Z.; Wang, H.; Qi, S.; Wu, D.; Huang, J.; Li, X.; Wang, C.; Ma, J. Structural Regulation Chemistry of Lithium Ion Solvation for Lithium Batteries. *EcoMat* **2022**, *4* (4), e12200. https://doi.org/10.1002/eom2.12200.
(56) Qian, Y.; Hu, S.; Zou, X.; Deng, Z.; Xu, Y.; Cao, Z.; Kang, Y.; Deng, Y.; Shi, Q.; Xu, K.; Deng, Y. How Electrolyte Additives Work in Li-Ion Batteries. *Energy Storage Mater.* **2019**, *20*, 208–215. https://doi.org/10.1016/j.ensm.2018.11.015.
(57) Pastor-Fernández, C.; Yu, T. F.; Widanage, W. D.; Marco, J. Critical Review of Non-Invasive Diagnosis Techniques for Quantification of Degradation Modes in Lithium-Ion Batteries. *Renew. Sustain. Energy Rev.* **2019**, *109*, 138–159. https://doi.org/10.1016/j.rser.2019.03.060.

(58) Birkl, C. R.; Roberts, M. R.; McTurk, E.; Bruce, P. G.; Howey, D. A. Degradation Diagnostics for Lithium Ion Cells. *J. Power Sources* **2017**, *341*, 373–386. https://doi.org/10.1016/j.jpowsour.2016.12.011.
(59) Edge, J. S.; O'Kane, S.; Prosser, R.; Kirkaldy, N. D.; Patel, A. N.; Hales, A.; Ghosh, A.; Ai, W.; Chen, J.; Yang, J.; Li, S.; Pang, M. C.; Bravo Diaz, L.; Tomaszewska, A.; Marzook, M. W.; Radhakrishnan, K. N.; Wang, H.; Patel, Y.; Wu, B.; Offer, G. J. Lithium Ion Battery Degradation: What You Need to Know. *Phys. Chem. Chem. Phys.* **2021**, *23* (14), 8200–8221. https://doi.org/10.1039/d1cp00359c.
(60) Bond, T.; Gauthier, R.; Gasilov, S.; Dahn, J. R. In-Situ Computed Tomography of Particle Microcracking and Electrode Damage in Cycled NMC622/Graphite Pouch Cell Batteries. *J. Electrochem. Soc.* **2022**, *169* (8), 080531. https://doi.org/10.1149/1945-7111/ac8a22.
(61) Ruff, Z.; Xu, C.; Grey, C. P. Transition Metal Dissolution and Degradation in NMC811-Graphite Electrochemical Cells. *J. Electrochem. Soc.* **2021**, *168* (6), 060518. https://doi.org/10.1149/1945-7111/ac0359.
(62) Jung, R.; Metzger, M.; Maglia, F.; Stinner, C.; Gasteiger, H. A. Oxygen Release and Its Effect on the Cycling Stability of LiNixMnyCozO2(NMC) Cathode Materials for Li-Ion Batteries. *J. Electrochem. Soc.* **2017**, *164* (7), A1361–A1377. https://doi.org/10.1149/2.0021707jes.
(63) Gilbert, J. A.; Shkrob, I. A.; Abraham, D. P. Transition Metal Dissolution, Ion Migration, Electrocatalytic Reduction and Capacity Loss in Lithium-Ion Full Cells. *J. Electrochem. Soc.* **2017**, *164* (2), A389. https://doi.org/10.1149/2.1111702jes.
(64) He, H.; Dong, J.; Zhang, D.; Hang, D.; Zhu, X.; Chang, C. Feasible Synthesis of NCM811 Cathodes with Controllable Li/Ni Cationic Mixing for Enhanced Electrochemical Performance via a Nano Grinding Assisted Solid-State Approach. *Int. J. Energy Res.* **2021**, *45* (5), 7108–7119. https://doi.org/10.1002/er.6296.
(65) Rowden, B.; Garcia-Araez, N. A Review of Gas Evolution in Lithium Ion Batteries. *Energy Rep.* **2020**, *6*, 10–18. https://doi.org/10.1016/J.EGYR.2020.02.022.
(66) Wandt, J.; Freiberg, A. T. S.; Ogrodnik, A.; Gasteiger, H. A. Singlet Oxygen Evolution from Layered Transition Metal Oxide Cathode Materials and Its Implications for Lithium-Ion Batteries. *Mater. Today* **2018**, *21* (8), 825–833. https://doi.org/10.1016/j.mattod.2018.03.037.
(67) An, S. J.; Li, J.; Daniel, C.; Mohanty, D.; Nagpure, S.; Wood, D. L. The State of Understanding of the Lithium-Ion-Battery Graphite Solid Electrolyte Interphase (SEI) and Its Relationship to Formation Cycling. *Carbon* **2016**, *105*, 52–76. https://doi.org/10.1016/j.carbon.2016.04.008.
(68) Lin, N.; Jia, Z.; Wang, Z.; Zhao, H.; Ai, G.; Song, X.; Bai, Y.; Battaglia, V.; Sun, C.; Qiao, J.; Wu, K.; Liu, G. Understanding the

Crack Formation of Graphite Particles in Cycled Commercial Lithium-Ion Batteries by Focused Ion Beam - Scanning Electron Microscopy. *J. Power Sources* **2017**, *365*, 235–239. https://doi.org/10.1016/j.jpowsour.2017.08.045.

(69) Guo, L.; Thornton, D. B.; Koronfel, M. A.; Stephens, I. E. L.; Ryan, M. P. Degradation in Lithium Ion Battery Current Collectors. *J. Phys. Energy* **2021**, *3* (3), 032015. https://doi.org/10.1088/2515-7655/ac0c04.

(70) Hu, D.; Chen, L.; Tian, J.; Su, Y.; Li, N.; Chen, G.; Hu, Y.; Dou, Y.; Chen, S.; Wu, F. Research Progress of Lithium Plating on Graphite Anode in Lithium-Ion Batteries. *Chin. J. Chem.* **2021**, *39* (1), 165–173. https://doi.org/10.1002/cjoc.202000512.

(71) Rosa Palacín, M. Understanding Ageing in Li-Ion Batteries: A Chemical Issue. *Chem. Soc. Rev.* **2018**, *47* (13), 4924–4933. https://doi.org/10.1039/C7CS00889A.

(72) Llewellyn, A. V.; Matruglio, A.; Brett, D. J. L.; Jervis, R.; Shearing, P. R. Using In-Situ Laboratory and Synchrotron-Based X-Ray Diffraction for Lithium-Ion Batteries Characterization: A Review on Recent Developments. *Condens. Matter* **2020**, *5* (4), 75. https://doi.org/10.3390/condmat5040075.

(73) P. Black, A.; Sorrentino, A.; Fauth, F.; Yousef, I.; Simonelli, L.; Frontera, C.; Ponrouch, A.; Tonti, D.; Rosa Palacín, M. Synchrotron Radiation Based Operando Characterization of Battery Materials. *Chem. Sci.* **2023**, *14* (7), 1641–1665. https://doi.org/10.1039/D2SC04397A.

(74) Atkins, D.; Capria, E.; Edström, K.; Famprikis, T.; Grimaud, A.; Jacquet, Q.; Johnson, M.; Matic, A.; Norby, P.; Reichert, H.; Rueff, J.-P.; Villevieille, C.; Wagemaker, M.; Lyonnard, S. Accelerating Battery Characterization Using Neutron and Synchrotron Techniques: Toward a Multi-Modal and Multi-Scale Standardized Experimental Workflow. *Adv. Energy Mater.* **2022**, *12* (17), 2102694. https://doi.org/10.1002/aenm.202102694.

(75) Li, H.; Guo, S.; Zhou, H. In-Situ/Operando Characterization Techniques in Lithium-Ion Batteries and Beyond. *J. Energy Chem.* **2021**, *59*, 191–211. https://doi.org/10.1016/j.jechem.2020.11.020.

(76) Xiong, R.; Pan, Y.; Shen, W.; Li, H.; Sun, F. Lithium-Ion Battery Aging Mechanisms and Diagnosis Method for Automotive Applications: Recent Advances and Perspectives. *Renew. Sustain. Energy Rev.* **2020**, *131*, 110048. https://doi.org/10.1016/j.rser.2020.110048.

(77) Waldmann, T.; Iturrondobeitia, A.; Kasper, M.; Ghanbari, N.; Aguesse, F.; Bekaert, E.; Daniel, L.; Genies, S.; Gordon, I. J.; Löble, M. W.; Vito, E. D.; Wohlfahrt-Mehrens, M. Review—Post-Mortem Analysis of Aged Lithium-Ion Batteries: Disassembly Methodology and Physico-Chemical Analysis Techniques. *J. Electrochem. Soc.* **2016**, *163* (10), A2149. https://doi.org/10.1149/2.1211609jes.

(78) Schlüter, N.; Novák, P.; Schröder, D. Nonlinear Electrochemical Analysis: Worth the Effort to Reveal New Insights into Energy Materials. *Adv. Energy Mater.* **2022**, *12* (21), 2200708. https://doi.org/10.1002/aenm.202200708.
(79) Barcellona, S.; Piegari, L. Effect of Current on Cycle Aging of Lithium Ion Batteries. *J. Energy Storage* **2020**, *29*, 101310. https://doi.org/10.1016/j.est.2020.101310.
(80) Yao, F.; Pham, D. T.; Lee, Y. H. Carbon-Based Materials for Lithium-Ion Batteries, Electrochemical Capacitors, and Their Hybrid Devices. *ChemSusChem* **2015**, *8* (14), 2284–2311. https://doi.org/10.1002/cssc.201403490.
(81) Geng, Z.; Thiringer, T.; Lacey, M. J. Intermittent Current Interruption Method for Commercial Lithium-Ion Batteries Aging Characterization. *IEEE Trans. Transp. Electrification* **2022**, *8* (2), 2985–2995. https://doi.org/10.1109/TTE.2021.3125418.
(82) Lacey, M. J. Influence of the Electrolyte on the Internal Resistance of Lithium−Sulfur Batteries Studied with an Intermittent Current Interruption Method. *ChemElectroChem* **2017**, *4* (8), 1997–2004. https://doi.org/10.1002/celc.201700129.
(83) Chien, Y.-C.; Liu, H.; Menon, A. S.; Brant, W. R.; Brandell, D.; Lacey, M. J. Rapid Determination of Solid-State Diffusion Coefficients in Li-Based Batteries via Intermittent Current Interruption Method. *Nat. Commun.* **2023**, *14* (1), 2289. https://doi.org/10.1038/s41467-023-37989-6.
(84) Chien, Y. C.; Menon, A. S.; Brant, W. R.; Brandell, D.; Lacey, M. J. Simultaneous Monitoring of Crystalline Active Materials and Resistance Evolution in Lithium-Sulfur Batteries. *J. Am. Chem. Soc.* **2020**, *142* (3), 1449–1456. https://doi.org/10.1021/jacs.9b11500.
(85) Epp, J. 4 - X-Ray Diffraction (XRD) Techniques for Materials Characterization. In *Materials Characterization Using Nondestructive Evaluation (NDE) Methods*; Hübschen, G., Altpeter, I., Tschuncky, R., Herrmann, H.-G., Eds.; Woodhead Publishing, 2016; pp 81–124. https://doi.org/10.1016/B978-0-08-100040-3.00004-3.
(86) Stanjek, H.; Häusler, W. Basics of X-Ray Diffraction. *Hyperfine Interact.* **2004**, *154* (1), 107–119. https://doi.org/10.1023/B:HYPE.0000032028.60546.38.
(87) You, Y.; Celio, H.; Li, J.; Dolocan, A.; Manthiram, A. Modified High-Nickel Cathodes with Stable Surface Chemistry Against Ambient Air for Lithium-Ion Batteries. *Angew. Chem. Int. Ed.* **2018**, *57* (22), 6480–6485. https://doi.org/10.1002/anie.201801533.
(88) Coelho, A. A. TOPAS and TOPAS-Academic: An Optimization Program Integrating Computer Algebra and Crystallographic Objects Written in C++. *J. Appl. Crystallogr.* **2018**, *51* (1), 210–218. https://doi.org/10.1107/S1600576718000183.

(89) *Rodríguez-Carvajal, J. (2001) Recent Developments of the Program FULLPROF, in Commission on Powder Diffraction (IUCr). Newsletter, 26, 12-19. - References - Scientific Research Publishing*. https://www.scirp.org/(S(i43dyn45teexjx455qlt3d2q))/reference/ReferencesPapers.aspx?ReferenceID=1479337 (accessed 2023-09-04).

(90) Vernon-Parry, K. D. Scanning Electron Microscopy: An Introduction. *III-Vs Rev.* **2000**, *13* (4), 40–44. https://doi.org/10.1016/S0961-1290(00)80006-X.

(91) Vlaica, G.; Olivi, L. EXAFS Spectroscopy: A Brief Introduction. *Croat. Chem. Acta* **2004**, *77* (3), 427–433.

(92) Christensen, C. K.; Karlsen, M. A.; Drejer, A. Ø.; Andersen, B. P.; Jakobsen, C. L.; Johansen, M.; Sørensen, D. R.; Kantor, I.; Jørgensen, M. R. V.; Ravnsbæk, D. B. Beam Damage in Operando X-Ray Diffraction Studies of Li-Ion Batteries. *J. Synchrotron Radiat.* **2023**, *30* (3), 561–570. https://doi.org/10.1107/S160057752300142X.

(93) Jia, C.; Wohlfeld, K.; Wang, Y.; Moritz, B.; Devereaux, T. P. Using RIXS to Uncover Elementary Charge and Spin Excitations. *Phys. Rev. X* **2016**, *6* (2), 021020. https://doi.org/10.1103/PhysRevX.6.021020.

(94) S. Rangarajan, S.; Sunddararaj, S. P.; Sudhakar, A. V. V.; Shiva, C. K.; Subramaniam, U.; Collins, E. R.; Senjyu, T. Lithium-Ion Batteries—The Crux of Electric Vehicles with Opportunities and Challenges. *Clean Technol.* **2022**, *4* (4), 908–930. https://doi.org/10.3390/cleantechnol4040056.

(95) Rezvanizaniani, S. M.; Liu, Z.; Chen, Y.; Lee, J. Review and Recent Advances in Battery Health Monitoring and Prognostics Technologies for Electric Vehicle (EV) Safety and Mobility. *J. Power Sources* **2014**, *256*, 110–124. https://doi.org/10.1016/j.jpowsour.2014.01.085.

(96) Attia, P. M.; Bills, A.; Brosa Planella, F.; Dechent, P.; dos Reis, G.; Dubarry, M.; Gasper, P.; Gilchrist, R.; Greenbank, S.; Howey, D.; Liu, O.; Khoo, E.; Preger, Y.; Soni, A.; Sripad, S.; Stefanopoulou, A. G.; Sulzer, V. Review—"Knees" in Lithium-Ion Battery Aging Trajectories. *J. Electrochem. Soc.* **2022**, *169* (6), 060517. https://doi.org/10.1149/1945-7111/ac6d13.

(97) Smith, A. J.; Fang, Y.; Mikheenkova, A.; Ekström, H.; Svens, P.; Ahmed, I.; Lacey, M. J.; Lindbergh, G.; Furó, I.; Lindström, R. W. Localized Lithium Plating under Mild Cycling Conditions in High-Energy Lithium-Ion Batteries. *J. Power Sources* **2023**, *573*, 233118. https://doi.org/10.1016/j.jpowsour.2023.233118.

(98) Matras, D.; Ashton, T. E.; Dong, H.; Mirolo, M.; Martens, I.; Drnec, J.; Darr, J. A.; Quinn, P. D.; Jacques, S. D. M.; Beale, A. M.; Vamvakeros, A. Emerging Chemical Heterogeneities in a Commercial 18650 NCA Li-Ion Battery during Early Cycling Revealed by Synchrotron X-Ray Diffraction Tomography. *J. Power Sources* **2022**, *539*, 231589. https://doi.org/10.1016/j.jpowsour.2022.231589.

(99) Sato, K.; Tamai, A.; Ohara, K.; Kiuchi, H.; Matsubara, E. Non-Destructive Observation of Plated Lithium Distribution in a Large-Scale Automobile Li-Ion Battery Using Synchrotron X-Ray Diffraction. *J. Power Sources* **2022**, *535*, 231399. https://doi.org/10.1016/j.jpowsour.2022.231399.

(100) Liu, X.; Xu, G. L.; Yin, L.; Hwang, I.; Li, Y.; Lu, L.; Xu, W.; Zhang, X.; Chen, Y.; Ren, Y.; Sun, C. J.; Chen, Z.; Ouyang, M.; Amine, K. Probing the Thermal-Driven Structural and Chemical Degradation of Ni-Rich Layered Cathodes by Co/Mn Exchange. *J. Am. Chem. Soc.* **2020**, *142* (46), 19745–19753. https://doi.org/10.1021/jacs.0c09961.

(101) Fang, S.; Yan, M.; Hamers, R. J. Cell Design and Image Analysis for in Situ Raman Mapping of Inhomogeneous State-of-Charge Profiles in Lithium-Ion Batteries. *J. Power Sources* **2017**, *352*, 18–25. https://doi.org/10.1016/j.jpowsour.2017.03.055.

(102) Wu, L.; Xiao, X.; Wen, Y.; Zhang, J. Three-Dimensional Finite Element Study on Stress Generation in Synchrotron X-Ray Tomography Reconstructed Nickel-Manganese-Cobalt Based Half Cell. *J. Power Sources* **2016**, *336*, 8–18. https://doi.org/10.1016/j.jpowsour.2016.10.052.

(103) Müller, S.; Eller, J.; Ebner, M.; Burns, C.; Dahn, J.; Wood, V. Quantifying Inhomogeneity of Lithium Ion Battery Electrodes and Its Influence on Electrochemical Performance. *J. Electrochem. Soc.* **2018**, *165* (2), A339. https://doi.org/10.1149/2.0311802jes.

(104) Danner, T.; Singh, M.; Hein, S.; Kaiser, J.; Hahn, H.; Latz, A. Thick Electrodes for Li-Ion Batteries: A Model Based Analysis. *J. Power Sources* **2016**, *334*, 191–201. https://doi.org/10.1016/j.jpowsour.2016.09.143.

(105) Xu, C.; Merryweather, A. J.; Pandurangi, S. S.; Lun, Z.; Hall, D. S.; Deshpande, V. S.; Fleck, N. A.; Schnedermann, C.; Rao, A.; Grey, C. P. Operando Visualization of Kinetically Induced Lithium Heterogeneities in Single-Particle Layered Ni-Rich Cathodes. *Joule* **2022**, *6* (11), 2535–2546. https://doi.org/10.1016/j.joule.2022.09.008.

(106) Mistry, A.; Heenan, T.; Smith, K.; Shearing, P.; Mukherjee, P. P. Asphericity Can Cause Nonuniform Lithium Intercalation in Battery Active Particles. *ACS Energy Lett.* **2022**, *7* (5), 1871–1879. https://doi.org/10.1021/acsenergylett.2c00870.

(107) Lin, F.; Nordlund, D.; M. Markus, I.; Weng, T.-C.; L. Xin, H.; M. Doeff, M. Profiling the Nanoscale Gradient in Stoichiometric Layered Cathode Particles for Lithium-Ion Batteries. *Energy Environ. Sci.* **2014**, *7* (9), 3077–3085. https://doi.org/10.1039/C4EE01400F.

(108) Barré, A.; Deguilhem, B.; Grolleau, S.; Gérard, M.; Suard, F.; Riu, D. A Review on Lithium-Ion Battery Ageing Mechanisms and Estimations for Automotive Applications. *J. Power Sources* **2013**, *241*, 680–689. https://doi.org/10.1016/j.jpowsour.2013.05.040.

(109) Liu, M.; Ren, Z.; Wang, D.; Zhang, H.; Bi, Y.; Shen, C.; Guo, B. Addressing Unfavorable Influence of Particle Cracking with a Strengthened Shell Layer in Ni-Rich Cathodes. *ACS Appl. Mater. Interfaces* **2021**, *13* (16), 18954–18960. https://doi.org/10.1021/acsami.1c05535.
(110) Mikheenkova, A.; Gustafsson, O.; Misiewicz, C.; Brant, W. R.; Hahlin, M.; Lacey, M. J. Resolving High Potential Structural Deterioration in Ni-Rich Layered Cathode Materials for Lithium-Ion Batteries Operando. **2022**. https://doi.org/10.26434/chemrxiv-2022-jf09w.
(111) Park, H.; Park, H.; Song, K.; Song, S. H.; Kang, S.; Ko, K.-H.; Eum, D.; Jeon, Y.; Kim, J.; Seong, W. M.; Kim, H.; Park, J.; Kang, K. In Situ Multiscale Probing of the Synthesis of a Ni-Rich Layered Oxide Cathode Reveals Reaction Heterogeneity Driven by Competing Kinetic Pathways. *Nat. Chem.* **2022**, *14* (6), 614–622. https://doi.org/10.1038/s41557-022-00915-2.
(112) Zhang, H.; May, B. M.; Omenya, F.; Whittingham, M. S.; Cabana, J.; Zhou, G. Layered Oxide Cathodes for Li-Ion Batteries: Oxygen Loss and Vacancy Evolution. *Chem. Mater.* **2019**, *31* (18), 7790–7798. https://doi.org/10.1021/acs.chemmater.9b03245.
(113) Yan, P.; Zheng, J.; Tang, Z.-K.; Devaraj, A.; Chen, G.; Amine, K.; Zhang, J.-G.; Liu, L.-M.; Wang, C. Injection of Oxygen Vacancies in the Bulk Lattice of Layered Cathodes. *Nat. Nanotechnol.* **2019**, *14* (6), 602–608. https://doi.org/10.1038/s41565-019-0428-8.
(114) Park, G.-T.; Ryu, H.-H.; Park, N.-Y.; Yoon, C. S.; Sun, Y.-K. Tungsten Doping for Stabilization of Li[Ni0.90Co0.05Mn0.05]O2 Cathode for Li-Ion Battery at High Voltage. *J. Power Sources* **2019**, *442*, 227242. https://doi.org/10.1016/j.jpowsour.2019.227242.
(115) Zhang, R.; Qiu, H.; Zhang, Y. Enhancing the Electrochemical Performance of Ni-Rich LiNi0.88Co0.09Al0.03O2 Cathodes through Tungsten-Doping for Lithium-Ion Batteries. *Nanomaterials* **2022**, *12* (5), 729. https://doi.org/10.3390/nano12050729.
(116) Hunter, J. C. Preparation of a New Crystal Form of Manganese Dioxide: λ-MnO2. *J. Solid State Chem.* **1981**, *39* (2), 142–147. https://doi.org/10.1016/0022-4596(81)90323-6.
(117) Rodrigues, M.-T. F.; Kalaga, K.; Trask, S. E.; Shkrob, I. A.; Abraham, D. P. Anode-Dependent Impedance Rise in Layered-Oxide Cathodes of Lithium-Ion Cells. *J. Electrochem. Soc.* **2018**, *165* (9), A1697. https://doi.org/10.1149/2.0611809jes.
(118) Wachs, S. J.; Behling, C.; Ranninger, J.; Möller, J.; Mayrhofer, K. J. J.; Berkes, B. B. Online Monitoring of Transition-Metal Dissolution from a High-Ni-Content Cathode Material. *ACS Appl. Mater. Interfaces* **2021**, *13* (28), 33075–33082. https://doi.org/10.1021/acsami.1c07932.
(119) Joshi, T.; Eom, K.; Yushin, G.; Fuller, T. F. Effects of Dissolved Transition Metals on the Electrochemical Performance and SEI Growth in

Lithium-Ion Batteries. *J. Electrochem. Soc.* **2014**, *161* (12), A1915. https://doi.org/10.1149/2.0861412jes.
(120) Liu, W.; Oh, P.; Liu, X.; Lee, M. J.; Cho, W.; Chae, S.; Kim, Y.; Cho, J. Nickel-Rich Layered Lithium Transition-Metal Oxide for High-Energy Lithium-Ion Batteries. *Angew. Chem. Int. Ed.* **2015**, *54* (15), 4440–4457. https://doi.org/10.1002/ANIE.201409262.
(121) Lin, R.; Bak, S.-M.; Shin, Y.; Zhang, R.; Wang, C.; Kisslinger, K.; Ge, M.; Huang, X.; Shadike, Z.; Pattammattel, A.; Yan, H.; Chu, Y.; Wu, J.; Yang, W.; Whittingham, M. S.; Xin, H. L.; Yang, X.-Q. Hierarchical Nickel Valence Gradient Stabilizes High-Nickel Content Layered Cathode Materials. *Nat. Commun.* **2021**, *12* (1), 2350. https://doi.org/10.1038/s41467-021-22635-w.
(122) Lin, Q.; Guan, W.; Meng, J.; Huang, W.; Wei, X.; Zeng, Y.; Li, J.; Zhang, Z. A New Insight into Continuous Performance Decay Mechanism of Ni-Rich Layered Oxide Cathode for High Energy Lithium Ion Batteries. *Nano Energy* **2018**, *54*, 313–321. https://doi.org/10.1016/j.nanoen.2018.09.066.
(123) Liu, B.; Wang, Z.-B.; Yu, F.-D.; Xue, Y.; Wang, G.; Zhang, Y.; Zhou, Y.-X. Facile Strategy of NCA Cation Mixing Regulation and Its Effect on Electrochemical Performance. *RSC Adv.* **2016**, *6* (110), 108558–108565. https://doi.org/10.1039/C6RA20146F.
(124) Purwanto, A.; Yudha, C. S.; Ubaidillah, U.; Widiyandari, H.; Ogi, T.; Haerudin, H. NCA Cathode Material: Synthesis Methods and Performance Enhancement Efforts. *Mater. Res. Express* **2018**, *5* (12), 122001. https://doi.org/10.1088/2053-1591/aae167.
(125) Yamamoto, Y.; Ohtsuka, M.; Azuma, Y.; Takahashi, T.; Muto, S. Cation Mixing in LiNi0.8Co0.15Al0.05O2 Positive Electrode Material Studied Using High Angular Resolution Electron Channeling X-Ray Spectroscopy. *J. Power Sources* **2018**, *401*, 263–270. https://doi.org/10.1016/j.jpowsour.2018.08.100.
(126) Jung, R.; Strobl, P.; Maglia, F.; Stinner, C.; Gasteiger, H. A. Temperature Dependence of Oxygen Release from LiNi0.6Mn0.2Co0.2O2 (NMC622) Cathode Materials for Li-Ion Batteries. *J. Electrochem. Soc.* **2018**, *165* (11), A2869. https://doi.org/10.1149/2.1261811jes.
(127) Geng, L.; Wood, D. L.; Lewis, S. A.; Connatser, R. M.; Li, M.; Jafta, C. J.; Belharouak, I. High Accuracy In-Situ Direct Gas Analysis of Li-Ion Batteries. *J. Power Sources* **2020**, *466*, 228211. https://doi.org/10.1016/j.jpowsour.2020.228211.
(128) Renfrew, S. E.; McCloskey, B. D. Quantification of Surface Oxygen Depletion and Solid Carbonate Evolution on the First Cycle of LiNi0.6Mn0.2Co0.2O2 Electrodes. *ACS Appl. Energy Mater.* **2019**, *2* (5), 3762–3772. https://doi.org/10.1021/acsaem.9b00459.
(129) Eldesoky, A.; Bauer, M.; Azam, S.; Zsoldos, E.; Song, W.; Weber, R.; Hy, S.; Johnson, M. B.; Metzger, M.; Dahn, J. R. Impact of Graphite Materials on the Lifetime of NMC811/Graphite Pouch Cells: Part I.

Material Properties, ARC Safety Tests, Gas Generation, and Room Temperature Cycling. *J. Electrochem. Soc.* **2021**, *168* (11), 110543. https://doi.org/10.1149/1945-7111/ac39fc.

(130) Charbonneau, V.; Lasia, A.; Brisard, G. Impedance Studies of Li+ Diffusion in Nickel Manganese Cobalt Oxide (NMC) during Charge/Discharge Cycles. *J. Electroanal. Chem.* **2020**, *875*, 113944. https://doi.org/10.1016/j.jelechem.2020.113944.

(131) Duda, L.-C.; Edström, K. Oxygen Redox Reactions in Li Ion Battery Electrodes Studied by Resonant Inelastic X-Ray Scattering. *J. Electron Spectrosc. Relat. Phenom.* **2017**, *221*, 79–87. https://doi.org/10.1016/j.elspec.2017.06.003.

(132) Luo, K.; Roberts, M. R.; Hao, R.; Guerrini, N.; Pickup, D. M.; Liu, Y. S.; Edström, K.; Guo, J.; Chadwick, A. V.; Duda, L. C.; Bruce, P. G. Charge-Compensation in 3d-Transition-Metal-Oxide Intercalation Cathodes through the Generation of Localized Electron Holes on Oxygen. *Nat. Chem. 2016 87* **2016**, *8* (7), 684–691. https://doi.org/10.1038/nchem.2471.

(133) Luo, K.; Roberts, M. R.; Guerrini, N.; Tapia-Ruiz, N.; Hao, R.; Massel, F.; Pickup, D. M.; Ramos, S.; Liu, Y.-S.; Guo, J.; Chadwick, A. V.; Duda, L. C.; Bruce, P. G. Anion Redox Chemistry in the Cobalt Free 3d Transition Metal Oxide Intercalation Electrode Li[Li0.2Ni0.2Mn0.6]O2. *J. Am. Chem. Soc.* **2016**, *138* (35), 11211–11218. https://doi.org/10.1021/jacs.6b05111.

(134) Kwon, T.; Choi, J. W.; Coskun, A. The Emerging Era of Supramolecular Polymeric Binders in Silicon Anodes. *Chem. Soc. Rev.* **2018**, *47* (6), 2145–2164. https://doi.org/10.1039/C7CS00858A.

(135) Wetjen, M.; Solchenbach, S.; Pritzl, D.; Hou, J.; Tileli, V.; Gasteiger, H. A. Morphological Changes of Silicon Nanoparticles and the Influence of Cutoff Potentials in Silicon-Graphite Electrodes. *J. Electrochem. Soc.* **2018**, *165* (7), A1503–A1514. https://doi.org/10.1149/2.1261807jes.

(136) Orendorff, C. J. The Role of Separators in Lithium-Ion Cell Safety. *Electrochem. Soc. Interface* **2012**, *21* (2), 61. https://doi.org/10.1149/2.F07122if.

(137) Klein, S.; Wrogemann, J. M.; van Wickeren, S.; Harte, P.; Bärmann, P.; Heidrich, B.; Hesper, J.; Borzutzki, K.; Nowak, S.; Börner, M.; Winter, M.; Kasnatscheew, J.; Placke, T. Understanding the Role of Commercial Separators and Their Reactivity toward LiPF6 on the Failure Mechanism of High-Voltage NCM523 || Graphite Lithium Ion Cells. *Adv. Energy Mater.* **2022**, *12* (2), 2102599. https://doi.org/10.1002/aenm.202102599.

(138) Liu, Z.; Jiang, Y.; Hu, Q.; Guo, S.; Yu, L.; Li, Q.; Liu, Q.; Hu, X. Safer Lithium-Ion Batteries from the Separator Aspect: Development and Future Perspectives. *ENERGY Environ. Mater.* **2021**, *4* (3), 336–362. https://doi.org/10.1002/eem2.12129.

(139) Lv, W.; Zhang, X. Chapter 10 - Recent Advances in Lithium-Ion Battery Separators with Enhanced Safety. In *60 Years of the Loeb-Sourirajan Membrane*; Tseng, H.-H., Lau, W. J., Al-Ghouti, M. A., An, L., Eds.; Elsevier, 2022; pp 269–304. https://doi.org/10.1016/B978-0-323-89977-2.00025-7.
(140) Sharma, G.; Jin, Y.; Lin, Y. S. Lithium Ion Batteries with Alumina Separator for Improved Safety. *J. Electrochem. Soc.* **2017**, *164* (6), A1184. https://doi.org/10.1149/2.1091706jes.
(141) Palacín, M. R.; de Guibert, A. Why Do Batteries Fail? *Science* **2016**, *351* (6273), 1253292. https://doi.org/10.1126/science.1253292.
(142) Chen, A.; Wang, K.; Li, J.; Mao, Q.; Xiao, Z.; Zhu, D.; Wang, G.; Liao, P.; He, J.; You, Y.; Xia, Y. The Formation, Detriment and Solution of Residual Lithium Compounds on Ni-Rich Layered Oxides in Lithium-Ion Batteries. *Front. Energy Res.* **2020**, *8*.

Acta Universitatis Upsaliensis

*Digital Comprehensive Summaries of Uppsala Dissertations from the Faculty of Science and Technology* 2329

Editor: The Dean of the Faculty of Science and Technology

A doctoral dissertation from the Faculty of Science and Technology, Uppsala University, is usually a summary of a number of papers. A few copies of the complete dissertation are kept at major Swedish research libraries, while the summary alone is distributed internationally through the series Digital Comprehensive Summaries of Uppsala Dissertations from the Faculty of Science and Technology. (Prior to January, 2005, the series was published under the title "Comprehensive Summaries of Uppsala Dissertations from the Faculty of Science and Technology".)

Distribution: publications.uu.se
urn:nbn:se:uu:diva-514588

ACTA UNIVERSITATIS
UPSALIENSIS
2023